

Groundwater Dynamics and Arsenic Contamination in Bangladesh

Charles F. Harvey^{1*}, Khandaker N. Ashfaque¹, Winston Yu¹, A. B. M. Badruzzaman², M. Ashraf Ali², Peter M. Oates¹, Holly A. Michael¹, Rebecca B. Neumann¹, Roger Beckie³, Shafiqul Islam⁴, M. Feroze Ahmed²

¹ *Parsons Laboratory, CEE, MIT, Cambridge, MA*

² *Bangladesh University of Engineering and Technology, Dhaka, Bangladesh*

³ *University of British Columbia, BC, Canada*

⁴ *Tufts University*

Abstract:

Although arsenic contaminated groundwater in Bangladesh is a serious health issue, little is known about the complex transient patterns of groundwater flow that flush solutes from aquifers and carry solutes into the subsurface. Hydrologic modeling results for our field site in the Munshiganj district indicate that groundwater flow is vigorous, flushing the aquifer over time-scales of decades to a century, and also transporting solute loads into the aquifer with recharge from ponds, rivers and rice fields. The combined hydrologic and biogeochemical results from our field site imply that the biogeochemistry of the aquifer system may not be in steady-state, and that the net effect of competing processes could either increase or decrease arsenic concentrations over the next decades. Modeling results suggest that irrigation has greatly changed the location, timing and chemical content of recharge to the aquifer, flushing water through the system more quickly, and also cycling large fluxes of water through rice fields during the dry season that could mobilize arsenic from oxides in near-surface sediments. Furthermore, the hydrologic model reveals that ponds, many of which have been excavated over the last fifty years, now provide much of the groundwater recharge. These ponds receive most of the waste from the villages and thus provide another potential source of organic carbon to the groundwater system.

Keywords: Arsenic, Groundwater, Bangladesh, Groundwater Modeling

1. Introduction

Over the last thirty years most of the population of Bangladesh and West Bengal switched their water supply from ponds and rivers to well water. As many as 10 million new domestic wells have been installed, providing drinking water for over 130 million people. Tragically, much of the region's groundwater is dangerously contaminated by arsenic and approximately 57% of these people now drink water with arsenic concentrations above 10 ppb, the standard of the World Health Organization [Yu et al., 2003]. Irrigation wells, mostly extracting from the shallow aquifer, were installed across the country concurrent with this transition of the domestic water supply. According to BADC (2003), a total of 924,023 shallow tubewells and 23,434 deep tubewells were used for irrigation in Bangladesh during the 2003 dry season, and groundwater irrigation covered about 75% of the total irrigated area. Groundwater irrigation greatly increased agricultural production enabling Bangladesh to become self-sufficient in food even though the population nearly tripled over the last four decades. Irrigation now sustains production of dry-season rice called Boro, which provides greater yields than the traditional rice grown during the wet season (Figure 1). During 2003 dry season, about 87% of the total irrigated area of about 4 million hectare (about 28% of the total area of the country) was under Boro cultivation and Boro accounted for about 49% of the total rice production (MoA, 2004). Thus, issues of groundwater quality and quantity have become vital for both the supply of drinking water and the production of food in Bangladesh.

A wide range of evidence indicates the importance of groundwater flow to the subsurface biogeochemistry in Bangladesh, however little work has been directed towards understanding the physical groundwater system. The hydrogeologic characterization that has been conducted across Bangladesh is small relative to that conducted at groundwater contamination sites in the US, for example, where groundwater is not used for drinking. This paper focuses on how groundwater flow and solute transport through Bangladeshi aquifers affects arsenic concentrations. We first describe the biogeochemical processes that control the aqueous/solid phase partitioning of arsenic in Bangladesh, and consider possible explanations for observed vertical profiles of chemical parameters within the aquifers. We then discuss the processes that drive groundwater flow in Bangladesh by analyzing hydraulic data we have collected from our field site in Munshiganj, which includes detailed diurnal and seasonal hydraulic head cycles, as well as seasonal water levels in ponds, rice fields and rivers, and budgets for irrigation pumping.

Finally, we use a lumped-parameter model of the groundwater system to show how irrigation pumping changes the source of recharge to the aquifers and reduces the residence time of groundwater by redirecting natural discharge from the rivers into irrigated rice fields and increasing recharge from ponds.

2. Biogeochemistry and Arsenic Mobility

Researchers agree that dissolved arsenic in the groundwater of Bangladesh originates from the sediments. However, there is no evidence of widespread, unusually high, levels of solid phase arsenic in the aquifer material -- concentrations are typically less than 10 ppm in sandy sediment and less than 100 ppm in clays and peats [Nickson et al., 1998; Swartz et al., 2004; McArthur et al., 2004]. Thus, it appears that high dissolved arsenic concentrations in groundwater are the result of particular hydrologic and biogeochemical conditions that partition arsenic from the solid to the aqueous phase and perhaps transport arsenic into contaminated aquifers, but have not yet flushed dissolved arsenic from these aquifers.

The original source of the arsenic was most likely oxidation of sulfide minerals, principally pyrite, derived from the granitic and metamorphic source regions of the Himalayas. In an accompanying paper in this issue, Polizzotto et al. [2004] shows that arsenic-bearing pyrite grains have reached the Ganges delta and are incorporated in the aquifers. This work supports the hypothesis that minerals are cyclically weathered near the land surface, where the water table rises and falls each year. When oxygen is introduced into the near surface, sulfide minerals are oxidized, iron oxides form, and arsenic is transferred from pyrite to iron oxides. During anoxic conditions, which may coincide with periods of recharge as return flow from rice fields, iron-oxides dissolve and arsenic is released into the water column where it is transported to depth with the recharge water. Previous researchers have suggested that pyrite oxidation occurred during weathering at the source in the Himalayas and that arsenic was transported and deposited in the Ganges delta in association with the resulting iron oxides [McArthur et al., 2004]. Some arsenic was likely transported into the Ganges Delta in both states, but the important difference between these two explanations is that the redox cycle scenario provides an explanation for a source of dissolved arsenic near the land surface, whereas the distributed iron-oxide explanation places the source of dissolved arsenic deeper within the aquifers.

The reducing conditions of almost all groundwater in Bangladesh (demonstrated by high

levels of dissolved ferrous iron and methane, and low measurements of Eh), and the weak but statistically-significant positive correlation of dissolved arsenic to iron and bicarbonate, suggest that most arsenic is liberated by dissolution of iron (oxy)hydroxides, or perhaps desorption of arsenic after reduction from arsenate to arsenite [Nickson et al., 1998; BGS and DPHE, 2001; Harvey et al., 2002]. The low concentrations of sulfate (and in some areas the negative correlation between arsenic and sulfate) as well as the generally reducing conditions indicate that arsenic has not been directly mobilized into groundwater from sulfide minerals [e.g., Harvey et al., 2002].

Microbiological processes drive many geochemical transformations in Bangladeshi soils and groundwater (see, for example Oremland and Stolz [2005]), and microbial activity likely ensures that the timescales of biochemical processes are much less (~weeks) than the residence times of groundwater (~decades). Laboratory batch experiments demonstrate that biotic [van Geen et al, 2004; Islam et al, 2004] and abiotic [Polizotto et. al., this issue] transformations occur within weeks or even hours, and these results are confirmed by field perturbation experiments [Harvey, 2002]. Consequentially, the rate of chemical transformations within aquifers is likely controlled by the rate that chemical loads are transported into the subsurface, not by the rates of microbiological activity. Because microbial activity quickly drives the geochemical system to a state approaching local equilibrium, groundwater mixing is the limiting process for chemical transformations within aquifers, as is typical of many groundwater systems. Because microbes are ubiquitous, understanding specific details of microbial enzymatic and metabolic pathways may prove important if: (1) Geochemical transformations near the land surface, where rapid water table movement may change chemical conditions on the time-scale of microbial response, prove to be important; (2) Evidence is found that significant transformations occur against a thermodynamic gradient, such as may result from detoxification; (3) Important microbial processes are found that occur only slowly, over the decades long time-scale of solute transport and mixing.

2.1. Geochemistry of Brown/Orange and Grey Sediment

Several research teams [BGS and DPHE, 2001; Harvey et al., 2002; McArthur et al., 2004; van Geen et al., 2003] describe two distinct types of aquifer sediment: brown (or orange to yellow) sediment presumably containing iron (oxy)hydroxides where dissolved arsenic concentrations in porewater are low, and grey sediments where dissolved arsenic concentrations

may be high. The brown sediments are found at depth in the older Pleistocene aquifers such as the Dupi Tila formation, where low-arsenic water is obtained, as well as near the surface. Dissolved arsenic is presumably low in these sediments because of the capacity of iron (oxy)hydroxides to adsorb arsenic. Islam et al. [2004] showed that arsenic is liberated from sediments collected in West Bengal by the addition of organic carbon. They do not report the *in-situ* arsenic concentrations in the pore-water, but the sample contains iron (oxy)hydroxides and is described as coming from a transition zone between a region of oxidizing conditions and a region with reducing conditions.

High concentrations (>200 ppm) of arsenic have been found in orange, (oxy)hydroxide-rich, bands ~1.5 m deep in soils [Breit, 2003] at several locations in the country. Such horizontal bands of iron oxides have previously been described in the soil science literature [Brammer, 1977] for Bangladesh, and indeed have provided the evidence for a soil development process termed ferolysis [Brammer, 1996; van Ranst, 2002] by which oxide layers develop. If such arsenic-rich iron bands prove to be ubiquitous, then their biochemical reduction could potentially provide an important source of dissolved arsenic into water that recharges the aquifers, consistent with the analysis of Polizotto et. al. [this issue].

The role played by iron (oxy)hydroxides within the contaminated grey sediments of the Holocene aquifer, where most wells withdraw water, is much more enigmatic. Iron (oxy)hydroxides must exist, or have existed very recently, according to the theory that arsenic is released from iron (oxy)hydroxides in local sediments by organic carbon oxidation. However these iron (oxy)hydroxides have not been definitively documented in the grey sediment and high concentrations of methane and hydrogen [Harvey et al., 2002] in strongly reducing water indicate that geochemical conditions are not conducive to stability of iron (oxy)hydroxides. Given that dissimilatory iron reduction, the primary means of iron reduction, precedes methane generation in sediment diagenesis, active iron reduction would most likely have occurred at an earlier stage in diagenesis as opposed to the present time. Furthermore, iron (hydr)oxides have not been detected in grey sediments from Munshiganj using either bulk- or micro-X-ray absorption spectroscopy (XAS), indicating that they comprise less than 5% of the total Fe [Polizotto et. al., this issue] and, in sequential extractions, all of the ferric iron can be accounted for as magnetite [Swartz et al., 2004] within experimental error. Thus, the role that iron (oxy)hydroxides may have played in controlling the current concentrations of dissolved arsenic

is difficult to determine.

Further complicating the puzzle over the role of iron (oxy)hydroxides, Swartz et al. [2004] show that only very small quantities would be required to explain the current ratio of sorbed to dissolved arsenic, and McArthur et al. [2004] provides a geologic explanation for why the Ganges Delta sediment would have been deposited with relatively little iron (oxy)hydroxides. Thus, it is conceivable that slow reductive dissolution within aquifer sediments could be responsible for high dissolved arsenic concentrations, but only if the geochemical system happens to be in a state where iron (oxy)hydroxides have released almost all of their sorbed arsenic. In other words, the aquifer sediments must be poised in a geochemical state where the inventory of iron (oxy)hydroxides is nearly (or recently) exhausted, yet arsenic has not been flushed away by flowing groundwater. Other explanations, that we explore below, are that both the physical flow system and the biogeochemical system have recently been perturbed, and that dissolved arsenic originates from near-surface sediments above the aquifer which may have a much larger composition of (oxy)hydroxides.

Dissolved arsenic concentrations are maintained in part because geochemical factors conspire to prevent arsenic that has been dissolved from sorbing back onto aquifer sediment. First, the paucity of ferric (oxy)hydroxides implies there may be few adsorption sites. Second, high concentrations of other anions, such as silicate and phosphate, which compete with arsenic for surface sorption sites, are prevalent in groundwater throughout most of the arsenic-affected areas. However, there is no convincing correlation between the concentrations of these anions and arsenic that would indicate that the spatial pattern of competing anions can explain the pattern of dissolved arsenic. Equilibrium chemical modeling using the parameters measured at our site indicates that silicate, phosphate and other anions compete, preventing arsenic from sorbing [Swartz et al., 2004]. These conceptual geochemical models are further complicated by the fact that arsenic likely adsorbs to surfaces of many solid phases other than oxyhydroxides, such as magnetite, green rust, and potentially siderite and apatite. Arsenic is known to sorb readily to magnetite [Dixit and Herring, 2003] and the results of our density and magnetic separations show that the magnetite fraction has the highest arsenic concentration by weight [Swartz et al., 2004].

2.3 Irrigation Pumping and Time Trends in Arsenic Concentration.

Several research groups postulate that irrigation pumping may flush arsenic from aquifers

[e.g. Harvey et al., 2003; McArthur et al., 2004]. Harvey et al. (2003) support this contention by comparing concentrations sampled from irrigation wells to concentrations from drinking water wells to show that irrigation wells, which flush much greater quantities of water, have significantly lower arsenic concentrations. At a national scale, Ali [2003] estimated that each year groundwater irrigation removes from aquifers, and then applies to fields, about one million kilograms of arsenic.

On the other hand, some evidence suggests that arsenic concentrations may rise after pumping commences. Kinniburgh et al. [2003], van Geen et al. [2003] and McArthur et al. [2004] all provide strong statistical evidence that arsenic concentrations in domestic well water correlate to the age of the well, suggesting that arsenic concentrations may rise after a well is installed, perhaps because irrigation wells, which have much greater effects on the local groundwater system, are installed in the region at the same time as the domestic wells where arsenic is measured. Can these apparently contradictory suggestions of both falling and rising arsenic concentrations be reconciled? Clearly pumping removes some arsenic from the aquifer. In fact, irrigation pumping can be viewed as analogous to “pump-and-treat” groundwater remediation methods employed in North America and Europe, but without the “treat” and with extraction rates that are actually higher than at many sites! However, increased flushing may be concurrent with increased input of dissolved arsenic, caused either by simple groundwater transport or by release driven by input of organic carbon from surface sources, or from sediments, including peat layers. This concurrent enhancement of both sinks and sources of arsenic to the groundwater system by human perturbation could potentially create very complex temporal and spatial behavior of dissolved arsenic.

At our site in Munshiganj, processes appear to be competing to both increase and decrease arsenic concentrations: arsenic is being extracted from the system and radiocarbon dating of dissolved carbon indicates that arsenic has been mobilized recently [Harvey et al., 2002]. The radiocarbon data show that detrital organic carbon has not driven recent biogeochemical reactions. The byproducts of microbial activity, both inorganic carbon and methane, have much younger radiocarbon dates than the dissolved organic carbon or the sediment, and the concentration of this inorganic carbon is much larger than that of the older organic carbon. In fact, at 20 m depth, the inorganic carbon has levels of carbon-14 higher than 100% modern. This is carbon from bomb testing, so it entered the aquifer in the last 50 years.

At three 30-m wells dissolved inorganic carbon (DIC) radiocarbon ages are 462, 770, and 823 years, much younger than the local sediment and the radiocarbon age of dissolved organic carbon (DOC) (3636, 1538, and 1890 years). Tree roots and burrowing animals are unlikely to penetrate below 10 m because the aquifer remains saturated all year, and in our discussion of the hydrologic model, we will consider whether roots in villages may penetrate through 6 m of clay to reach the aquifer. Thus, dissolved carbon with a radiocarbon age younger than the sediment age was transported downward and laterally by flowing groundwater.

The presence of young DIC and old DOC in the same water does not appear to result from the mixing of young, DIC-containing water and old, DOC-containing water. The concentrations correlate strongly (i.e. water high in young DIC is also high in old DOC); they do not follow a mixing-line that would have a negative correlation. Thus it appears that the older DOC was mobilized from the sediment concurrently with the production or inflow of young DIC. McArthur et al. [2004] argue that buried peat deposits have provided the organic carbon that drives reduction at our field site, but they do not attempt to reconcile the different radiocarbon ages of dissolved organic carbon and inorganic carbon.

3. Geochemical Profiles with Depth

In this section, we consider how geochemical characteristics vary with depth in aquifers, and hence how chemical conditions relate to flow paths and groundwater age. Figure 2 compares depth profiles of solute concentrations measured at our field site in Munshiganj with averaged values from the BGS and DPHE [2001] data set. Our site in the Munshiganj district (Figure 3) is located 30 km south of Dhaka and 7 km north of the Ganges. It contains a small intensive-study area (100 m²) with 25 sampling wells (Figure 3B) that extract water from depths ranging between 5 to 165 m below the land surface (Figure 4B). We also monitor water levels at 87 other locations in the surrounding 16-km² region. We describe some similarities between results at our single site and the averaged national data set that suggest some general characteristics of geochemical evolution and transport across the region.

3.1 Arsenic as a function of depth

At the site in Munshiganj, dissolved arsenic has a distinct peak at approximately 30 m depth, but we find no chemical characteristic of the solid sediment to explain this pattern [Harvey et al., 2002; Swartz et al., 2004]. The geochemistry of the local sediment and the

dissolved components in the groundwater and indicate an arsenic source that is hydrologically upgradient. Furthermore, several types of data, when taken together, suggest a relation between the arsenic peak and groundwater flow patterns.

The pumping-test hydraulic conductivity estimates (Figure 4A) indicate that a lower conductivity layer at 24 m may partially separate horizontal flow paths at our small intensive study site. Higher conductivity strata are evident at 18 m and 60 m, and at 24 m the well has suffered significant silting, so that the estimated conductivity value is uncertain, but appears to be much lower than above or below. The head data (Figure 4B) show that, at least during some times of year, there is convergent vertical flow that mixes water from above and below 38 m, indicating that horizontal flow must accelerate to conserve mass at this depth. Evidence for groundwater mixing at 30 m is supported by the O-18 profile (Figure 4C). The range of isotope ratios at 30 m is consistent with mixing of lighter water from above and heavier water from below. The heavier water below 30 m could represent infiltrated pond, river or rice-field water that has been subject to relatively more evaporation. Measurable tritium was found to 30 m depth and at 60 m, where hydraulic conductivity appears highest (although not between 30 and 60 meters) [Harvey et al., 2003]. These values indicate the presence of at least a component of water that is less than 40 years old. Furthermore, the tritium values show a sharp decrease to less than 1 T.U. below 24 m, so that the peak of high dissolved arsenic corresponds with the depth where older water mixes with younger recharge. We do not have detailed data beyond our small intensive study site to extrapolate these results to the region.

An obvious possibility for the recharge source of the shallow groundwater at our intensive study site is the neighboring pond (figure 3B, P-1). Ponds lose water at a faster rate than potential evaporation and maintain a hydraulic gradient towards our sample wells. However, the cause of the variable O-18 ratios (Figure 4C) is unknown, and we do not currently have a sufficient transient 3D characterization of the flow field to support this hypothesis.

Kinniburgh et al. [2003] and McArthur et al. [2004] both describe typical depth profiles of arsenic concentrations as “bell shaped”. Although the general trend of decreasing arsenic levels with depth is obviously evident from the national data set (Figure 2) the upper part of the “bell shape”, increasing arsenic with depth, is not statistically robust for the combined data set and is only evident in histograms when certain bin intervals are chosen. However the “bell shaped” pattern is evident at a variety of specific study sites [Harvey et al., 2002; McArthur et al., 2004;

van Geen et al., 2003]. Depth trends can also be considered within different geologic regions, and Yu et al. [2003] tabulate the geologic regions of Bangladesh where there is a statistically significant trend of decreasing arsenic with depth (they did not consider non-monotonic trends). Their geostatistical analysis shows that the trend of decreasing arsenic concentrations with depth explains much of the differences in arsenic concentrations between nearby wells: neighboring wells often have different arsenic levels because one withdraws water from deeper in the aquifer where arsenic concentrations are lower.

3.2. Sulfate, Calcium and Ammonium as a Function of Depth

At the Munshiganj site, the inverse relation of dissolved sulfate with As (Figure 2), and the presence of acid volatile sulfide (AVS) in the sediments near the dissolved As peak, suggest that arsenic has not been released directly by sulfide oxidation. Instead, low dissolved sulfur levels appear to limit the precipitation of sulfides near the arsenic peak. The BGS and DPHE [2001] countrywide data set also shows a distinct, statistically robust, pattern of decreasing sulfate with depth. This rapid decline of sulfate with depth is consistent with the previously described scenario for input by cyclical sulfide weathering with water-table oscillations, followed by sulfate reduction in the aquifer. Furthermore, monthly measurements of sulfate by the BGS and DPHE [2001] in very shallow dug wells are also consistent with this scenario, with some containing very high concentrations with seasonal oscillations.

At our site, peaks in ammonium and calcium mirror the sharp peak in arsenic (Figure 2), and these solutes suggest inflow and oxidation of organic carbon, and subsequent mixing of solutes. Ammonium is an oxidation product of natural organic matter, and calcium may be released from solid carbonate after organic carbon oxidation [Swartz et al., 2004]. Furthermore, dissolved organic carbon, with radiocarbon ages in accord with estimated sediment ages, also shows a bell shaped profile, indicating that recalcitrant detrital organics may have been liberated from sediment concurrent with the processes that liberate arsenic. The BGS and DPHE [2001] do not report ammonium for their countrywide data set, but the profile of calcium with depth appears to show a “bell shape” similar to that found at our site.

3.3. “Bell Shaped” Depth Profiles

The bell shaped pattern of solutes (arsenic, ammonium, calcium, and dissolved carbon) with depth is typical of vertical profiles of contaminant plumes that originate from localized surface sources before moving laterally and downward into aquifers. After solute enters an

aquifer, a plume migrates laterally away from this source location and is pushed deeper into the aquifer by recharge from above. Thus, the basic hydrologic process of lateral transport creates vertical profiles of contamination with typical “bell” shapes. Such profiles have been characterized on multitudes of groundwater contamination sites in North America and Europe where release of pollutants at distinct surface locations contaminates groundwater as migrating plumes.

Simple geometric considerations indicate that groundwater fluxes at our site have a large lateral component, consistent with conventional understanding for horizontal alluvial aquifer systems [Freeze and Witherspoon, 1966]. After water enters the aquifer from the surface, it must move laterally to reach discharge areas. At our site, the lateral velocity component must be relatively large in much of the aquifer because the spacing between discharge areas, irrigation wells and river channels, is as great or greater than the thickness of the aquifer (~100 m). Furthermore, at the location of our intensive study site, where the geochemical profiles were characterized, there is no irrigation well beneath our sampling piezometers; without such a sink at depth, the convergence of vertical flow indicated by our head gradients and isotope data must be accommodated by accelerating horizontal flow.

Thus, the average vertical component of flow in recharge areas determines the net chemical flux from the surface down into the aquifer, and the 3-D pattern of groundwater flow determines the pattern of solute migration from the sources. While one can postulate that the bell-shaped pattern at our site results from a particular local source of organic carbon (i.e. a nearby pond, river or rice field), it remains an open question whether the much less distinct bell-shaped pattern of the national BGS and DPHE [2001] data, or similar patterns observed at other small-scale sites, results from the same mechanisms. It is intriguing that the bell-shape pattern of arsenic is mirrored by the distribution of well depths (not shown) in the BGS and DPHE [2001] data set. Most wells withdraw water from depths near 25 m. Similarly, at our site in Munshiganj nearly all wells (drinking and irrigation) are completed at the same depth where we find the arsenic peak, 30 m. This correspondence may suggest a hydraulic component to the cause of arsenic mobility with depth. Because deeper wells are more expensive, villagers complete wells only to a depth sufficient to provide adequate yield, perhaps below the low conductivity layer we find at 24 m (Figure 4). Thus, a relationship may exist between the depth at which the aquifer becomes more conductive to groundwater flow, and the depth of maximum arsenic concentration.

However, such speculation has not been confirmed by detailed hydrogeologic studies.

The correspondence of the depth profiles measured at our site to the average BGS and DPHE [2001] profiles should not be interpreted as indicating that the same processes are occurring everywhere. There is spatial heterogeneity in aqueous chemical characteristics, much of which is likely induced by the complex mosaic of recharge and discharge areas at the surface which have variable water chemistry. However, the correspondence does suggest the existence of dominant reactive-transport processes that affect the subsurface biogeochemistry at many locations across the country.

One interesting observation from our site is that the stable water isotopes indicate a transition between surface sources of recharge that corresponds with the arsenic peak. Thus, it is possible that the high arsenic values at the peak are caused by the mixing of groundwater from two different sources, rather than the input from one particular source. This points to the need to identify sources of recharge at our site.

4. The Relation of Groundwater Flow and Chemical Transport to Arsenic Concentrations

Much of the existing literature on groundwater flow in Bangladesh focuses on isotopic inference, and not on physical understanding of flow and solute transport. However, several simple lines of reasoning, and some isotope data, indicate that flow and transport play important roles in subsurface arsenic concentrations.

4.1. Irrigation Pumping

Figure 1 indicates that, at a national level, pumping alone drives significant groundwater flow. Boro rice requires ~1 meter of irrigation annually [Hossain et al., 2003], and roughly 20% of the country cultivates groundwater irrigated Boro. Therefore, assuming a porosity of 20%, this withdrawal cycles 5 m of groundwater flow annually below rice fields, which amounts to 1 m of vertical groundwater circulation when averaged over the non-irrigated areas. Thus, pumping-induced groundwater flows reach depths of 20 or 30 meters within two or three decades, on average. (Of course, pumping-induced flow is much greater in the vicinity of irrigation wells and will not be evenly distributed, but somewhat channeled into higher-conductivity pathways.)

Some researchers have suggested that pumping does not greatly change groundwater flow because natural flow is already rapid [Aggarwal et al., 2003]. Pumping must change the

pattern of flow because it introduces spatially distinct sinks (well screens) into the groundwater system, altering the 3-D flow paths of groundwater. Because hydraulic heads are described by a 3-dimensional parabolic differential equation, inserting a sink in the system will change heads, and hence flow throughout the domain. Groundwater flow is not like rapid river flow; extracting groundwater changes the gradients everywhere, including up-gradient flow.

However, it is possible that pumping would not greatly change the average residence time of groundwater in the aquifer. Irrigation extraction could be offset by decreased natural discharge to rivers during the dry season. Although pumping must change groundwater flow paths, it would not change the average residence time if there was no return flow (re-infiltration of irrigation water) and if total irrigation withdrawals equaled the reduction in discharge to the rivers. Outflow from the system would simply be switched from discharge to rivers to increased evapotranspiration from crops. Such a scenario assumes perfectly efficient irrigation (i.e. no return flow) and an exact tradeoff between discharge to rivers and pumping. However, since there is return flow, there must be an increase in flow through the system (i.e. reduction in average residence time) even if the pumping withdrawal is offset by a decrease in discharge to the river. In the hydrologic modeling sections below, we address this question directly by estimating fluxes with and without irrigated agriculture.

4.2 Groundwater Tritium

Measured tritium values indicate groundwater flow through at least the upper 30 meters is often rapid. Measurable values of tritium ($\sim > 0.1$ T.U.) indicate that at least a component of the groundwater precipitated in the last 50 years, during which time atomic bomb testing greatly increased atmospheric level of tritium. The largest set of tritium data has been gathered by the IAEA [Aggarwal et al., 2002] over the last thirty years and their final report concludes that groundwater ages in the upper 100 m are generally less than 100 years. Their recent plot [Aggarwal et al., 2003] shows a somewhat more complex picture, with tritium values greater than 1 tritium unit (TU) penetrating below 25 m in 1999, but not in 1979. At our site, we also find tritium values above 0.2 TU to a depth of 60 m indicating a component of water less than 40 years. Clearly some areas of stagnant water [van Geen et al., 2003, Dowling, 2003] exist, either because of low hydraulic conductivity (e.g. clay layers) or because of local recharge and discharge patterns. However, the common occurrence of measurable tritium in groundwater indicates that groundwater flow is sufficient to rapidly transport arsenic, or solutes that interact

with arsenic, through large portions of the shallow aquifers where high arsenic concentrations are found.

Irrigation return flow, which now comprises a significant component of groundwater recharge, poses a challenge for the interpretation of tritium and helium measurements in contemporary groundwater. Because irrigation return flow is recycled groundwater, it has different tritium concentrations than precipitation, and may have very low tritium concentrations. Irrigation water is often withdrawn from below 30 m, and available data indicate that tritium levels can be low beneath this depth. Helium concentrations in return flow also may differ from precipitation if they have not equilibrated with the atmosphere before the water re-enters the subsurface.

We know of no measurements of either the tritium or helium concentrations in irrigation return flow. However, we can gain insight into how irrigation return flow may affect tritium-helium dating by considering several possible scenarios. First, the tritium concentrations in return flow may be below detection, and the helium may have re-equilibrated with the atmosphere in the rice fields. When this type of water is mixed with resident groundwater in the subsurface, it dilutes both the tritium and helium equally, so the ratio, from which the age is calculated, remains the same; thus the estimated tritium-helium age remains unchanged, although the helium concentration is reduced. A second possibility is that helium does not equilibrate with the atmosphere. In this case, low-tritium return flow will simply appear to be old groundwater. These two examples both show that tritium and helium concentrations may not distinguish irrigation return-flow from resident groundwater.

4.3. Patchiness of Dissolved Arsenic

Arsenic concentrations are extremely patchy over small spatial scales. In the vertical dimension, high concentrations can be found within tens of meters of low concentrations. If there is any groundwater flow across these concentration gradients, arsenic will be transported from areas of high concentrations to areas of low concentration, and vice versa. If flow does not cross these arsenic gradients, then the patchy spatial pattern of dissolved arsenic must correspond to the spatial pattern of groundwater flow paths. In either case, understanding the effects of flow and transport is important for understanding the behavior of dissolved arsenic; groundwater is either transporting arsenic, or the spatial pattern of flow paths is related to the spatial pattern of dissolved arsenic.

The complex mosaic of recharge and discharge areas at the surface provide one simple potential explanation for this spatial complexity in the subsurface. Because the topography is essentially flat, local flow systems dominate. Discharge areas (irrigation wells and rivers) and likely recharge areas (pond, rice fields, and rivers) are all spaced within tens and hundreds of meters of each other as demonstrated by the satellite image in Figure 3. This spacing of sinks and sources drives groundwater flow through a complex transient 3-dimensional system of flow paths which also must have spatial scales of tens and hundreds of meters.

4.4. Why is Dissolved Arsenic Still in the Groundwater?

The short residence time (decades) of some contaminated groundwater, as indicated by both tritium concentrations and pumping rates, suggests that arsenic is being flushed from the system. Indeed, estimated groundwater ages, and the rates of pumping-induced circulation described above, combined with the low estimated retardation coefficients for arsenic, raises the question of how such high concentrations of dissolved arsenic can remain in the groundwater. Kinniburgh et al. [2003] estimates the retardation factor for arsenic to be as low as two. We also find that, where arsenic is high, the effective retardation factor is less than ten [Harvey et al., 2002; Swartz et al., 2004]. These values imply a residence time for arsenic of decades to centuries in aquifers that are thousands of years old. So why is the arsenic still there? Possible explanations include: (1) Groundwater flow has not been rapidly flushing aquifers during past centuries, but rather is the result of the recent advent of massive irrigation; (2) Geochemical conditions have recently shifted to mobilize arsenic in greater concentrations, or; (3) Dissolved arsenic is provided hydrologically upgradient of the sampling wells by the near-surface process described in Polizzotto et al. [this issue]. We suspect that aspects of all three explanations apply to varying degrees at different locations, and that their relative importance will only be elucidated when the groundwater flow system is better understood.

5. The Annual Cycle of Groundwater Flow in Central Bangladesh

Discharge and recharge of groundwater follows a dramatic annual cycle, with floodwater returning the aquifer to full conditions every year. After floodwaters recede in the fall, groundwater is lost both by discharge to rivers and by evapotranspiration, which is enhanced by irrigation pumping. Then in the early summer, groundwater is recharged by direct rainfall, and by rising river levels.

5.1 Hydrologic Characteristics of the Munshiganj Field Site

Here we present hydrologic data that characterize the annual cycle of water levels at our field site and demonstrate several features of groundwater flow that are important for arsenic mobilization and transport. Figure 3B shows a map of a region within our larger study area. The hydrostratigraphy of our site (Figure 4) is representative of the deltaic depositional environment that is pervasive in Bangladesh and West Bengal [Khan, 2000]. The surface landscape consists of: (1) organic-rich clay/silt-lined fields; (2) ponds that are several meters deep with low-permeability clay bottoms; (3) villages and roads, rising 2 – 3 m above the level of the fields, that are constructed on clay/silt borrowed to excavate the ponds; (4) and the Ichamati River, which traverses the site and eventually flows into the Ganges approximately 7 km away. The surface overbank clay/silt deposit extends to a depth of approximately 3 m below ground surface, and acts as a confining or semi-confining layer to the underlying sand aquifer. The approximately 80 – 100 m thick sand aquifer is fairly homogeneous at our site, although localized peat and silts have been reported in other locations [Rahman and Ravenscroft, 2003; McArthur et al., 2004]. Groundwater wells are completed in this aquifer, most screened at around 30 m depth, where arsenic concentrations appear to be highest, with some irrigation wells screened deeper.

According to BADC (2002), about 45% of the total area (203 sq. km.) of Sreenagar Thana, where our field site in Munshiganj is located, was irrigated during the 2002 dry season. Of this total area, 52 km² (or about 26% of the total area of the Thana) was irrigated by 996 shallow irrigation wells, 3 km² was irrigated by 12 deep wells, and 37 km² by surface water using 223 low lift pumps (LLP). Thus there are about 5 irrigation wells per sq. km. area of the Thana and each shallow irrigation well covers about 0.053 km² of agricultural land. It should be noted that significantly higher density of irrigation wells could be found in the northern and in some southwestern districts of Bangladesh (Ali, 2003), where groundwater is easily available at shallow depth and availability of surface water for irrigation during the dry season is extremely limited. For example, in Dhunat Thana of the northern district of Bogra there are about 34 shallow irrigation wells per sq. km. of the Thana and each shallow well covers about 0.02 km² of agricultural land (BADC, 2002).

Annual hydrographs for irrigation wells, domestic wells, ponds, and the river are presented in Figure 5A for the 14 months from May 2003 to June 2004. Some basic features of these water levels are the following: (1) During monsoon flooding, all water levels and hydraulic heads

become much closer than the rest of the year. Because the head differences are relatively small, and the only pumping is domestic (irrigation ceases), flow is greatly reduced during flooding. (2) As the flood recedes, but before irrigation begins, the river level drops more quickly than the groundwater level, which drops more quickly than pond levels. (3) When irrigation begins in January, the decline of the river level slows but groundwater decline accelerates such that the hydraulic head in the aquifer falls below that in the river. (4) When monsoon flooding begins in June, all water levels rise rapidly together as the aquifer is recharged and both river water and rain inundate the land.

Our water-level observations allow us to develop a conceptual model of water flow in the vicinity of our field site. Generally, recharge enters the subsurface through pond and river bottoms, and the overlying confining unit, into the aquifer below. Undisturbed, the water would then flow laterally out to discharge into the rivers, or be drawn up by transpiration. Indeed, the drop in water levels in the aquifer after flooding recedes in December, but before irrigation pumping, is largely caused by discharge to the river.

The groundwater levels recorded every hour at our intensive study area (Figure 5B) show that beginning in January, irrigation pumping greatly changes flow in the system. At the onset of irrigation pumping, the rate at which groundwater heads decline doubles, and dramatic diurnal head oscillations develop as pumps are turned on during the day and off at night. The dramatic diurnal head differences demonstrate that the aquifer is confined, or semi-confined. Also in the beginning of January, the river reverses flow direction and no longer discharges to the Ganges, but rather flows, at a relatively low rate, from the Ganges to the field area.

While spatial gradients in the aquifer are very small, temporal fluctuations, caused by irregular pumping schedules, are more significant and spatially extensive, consistent with the high transmissivity of the aquifer. Heads recorded in different wells at approximately the same time rarely differ by more than several centimeters, yet the effect of the seasonal trend over a day is more than a centimeter and the daily oscillation from irrigation pumping can be more than 20 cm. From a practical point of view, this makes it very difficult to map groundwater flow directions. In the time required to walk from one well to another, the head in both wells may change by an amount larger than the instantaneous difference in head between the two wells. Thus, groundwater flow patterns are not readily apparent from the water level data in Figure 3 and are a focus of current 3-D numerical modeling.

5.2. Dynamic Lumped-Parameter Model of the Munshiganj Aquifer

Here we construct a dynamic model of recharge and discharge from the aquifer (Figure 7). We use this model to estimate the fluxes between the aquifer and the river, ponds, rice fields and villages, flows that cannot all be explicitly calculated from the data. First we use the model to estimate unknown hydrologic parameters. Then we apply the calibrated model to estimate the various fluxes in and out of the aquifer, with and without pumping, and to characterize the uncertainty in these fluxes given current data.

We use a lumped-parameter, or box, model that does not consider spatial gradients within the aquifer. This modeling choice is supported by the facts that: (1) Temporal gradients in hydraulic head overwhelm spatial gradients within the aquifer over both the annual cycle and the daily cycle, and; (2) Spatial gradients within the aquifer are too small to be measured by conventional methods, but gradients between the aquifer and surface water bodies are larger. The lumped-parameter model (Figure 6) couples the mass-balance equation for the aquifer with mass-balance equations for irrigated fields, ponds, and non-irrigated areas (mostly villages and roads):

Aquifer:

$$S \frac{dh_a}{dt} = (h_f - h_a)k_f f_f + (h_p - h_a)k_p f_p + (h_r - h_a)k_r f_r + (h_v - h_a)k_v f_v - q_l - f_{av} \alpha_v ET_0 \quad (1)$$

Village:
$$S_y \frac{dh_v}{dt} = (h_a - h_v)k_v - (1 - f_{av}) \alpha_v ET_0 + R \quad (2)$$

Field:
$$S_y \frac{dh_f}{dt} = (h_a - h_f)k_f - \alpha_f ET_0 + R + \frac{q_l}{f_f} \quad (3)$$

Pond:
$$\frac{dh_p}{dt} = (h_a - h_p)k_p - \alpha_p ET_0 + R \quad (4)$$

The following time-varying model output was fit to observed values to estimate the system parameters:

h_a	head in the aquifer [L]
h_f	head (water level) in the rice fields [L]
h_p	head (water level) in the ponds [L]
h_v	head in the non-irrigated areas (e.g. villages) [L]

The following time series were set to measured data values:

h_r	the river stage, a function of time [L]
q_i	the pumping rate $\left[\frac{L}{T}\right]$
ET_0	the reference crop evapotranspiration $\left[\frac{L}{T}\right]$
R	the rainfall rate $\left[\frac{L}{T}\right]$

The following system parameters were estimated in all cases:

k_r	hydraulic conductance between the river and the aquifer $\left[\frac{1}{T}\right]$
k_f	hydraulic conductance between the rice fields and the aquifer $\left[\frac{1}{T}\right]$
k_p	hydraulic conductance between the ponds and the aquifer $\left[\frac{1}{T}\right]$
k_v	hydraulic conductance between the non-irrigated areas and the aquifer $\left[\frac{1}{T}\right]$

The following dimensionless parameters were fixed to independently estimated values in all cases:

α_v	the scaling factor for non-irrigated area transpiration (i.e. trees)
α_f	the scaling factor for rice field evapotranspiration
α_p	the scaling factor for pond evaporation (i.e. pan evaporation)
S	Storativity of Aquifer
S_y	specific yield of near-surface clay (This value is set to 1 when the head is above the land surface indicating standing water in the rice fields.)
f_f	fraction of area covered by fields (65%)
f_p	fraction of area covered by ponds (10%)
f_v	fraction of area covered by nonirrigated areas (e.g. villages; 22%)
f_r	fraction of areas covered by rivers (2%)
f_{av}	aquifer-clay partition coefficient (fraction of ET_{tree} coming out of aquifer)

The left side of the aquifer equation describes the change in storage in the aquifer. The first four terms on the right side describe exchange with irrigated fields, ponds, the river, and non-irrigated areas, respectively. The final two terms represent pumping and transpiration from trees that may extend some roots into the aquifer. The hydraulic conductances (not conductivities) used in the model characterize the flow rate per unit area between two model

reservoirs. For example the flow rate between the field and aquifer is $Q_f = k_f(h_f - h_a), \left[\frac{L^3}{T} \right]$.

The transient mass balance equations for the fields, ponds and non-irrigated areas are each coupled to the mass balance equation for the aquifer through the hydraulic head in the aquifer, h_a . Because the water level in the river is controlled by the Ganges level (as discussed below) it is prescribed by the measured water levels, and there is no mass balance equation for the river. In the next sections we describe how our field data were used to construct the lumped parameter model.

5.2.1. Rates of Groundwater Extraction

We determined extraction rates for our study area by combining direct measurements of instantaneous pumping rates from local irrigation wells with the extraction schedule estimated from daily oscillations in aquifer hydraulic head. We then apply these pumping rates to the mass balance equations in order to model seasonal hydrological fluxes. Figure 7 shows a histogram of the measured instantaneous pumping rates from 41 of the 54 irrigation wells we have identified in the area surrounding our field site shown in Figure 3A. Our average measured rate of 24.1 L/sec is consistent with the range recently published by Shankar et al. [2004 (accepted)], but significantly greater than the value of 15 L/s cited in older reports for shallow irrigation pumps [Rahman and Ravenscroft, 2003]. The daily extraction was then computed as the average pumping rate multiplied by both the number of wells in use and the duration of pumping. As we discuss next, the last two quantities were estimated from observed water level fluctuations recorded by our automatic pressure transducers. Our calculations are applied specifically to a circular area with a 1.5 km radius centered at our intense field area (Figure 3A) that contains 32 irrigation wells. This area is large enough to be representative of a typical area; it contains many ponds, irrigation wells and a small river.

Irrigation pumping causes both daily fluctuations in groundwater heads (pumps are typically run from about 9 in the morning until 7 or 8 in the evening), and a secular decline in heads that is the accumulated effect of extraction over the season. Both the daily and the seasonal fluctuations are clearly visible in the hydrograph shown in Figure 8A. The daily duration of pumping can be determined from the hydrograph as the time between the peak head at the start of daily pumping, and the minimum head at the end. These daily oscillations are shown in Figure 8B after a 24 hr moving average is subtracted from the hydrograph to remove the effects the long-term seasonal decline, and precipitation and recharge. The magnitude of the oscillations show that the net extraction increases in January, the first month of the irrigation season, and then begins to decrease during April, with much less pumping in early May. Figure 8C shows that the daily duration of pumping is nearly constant at around 10 hours. Thus, it appears that the total daily extraction is controlled more by the number of wells pumping than by the hours of operation, a finding that is consistent with our own observations of local practices.

We used the magnitude of the daily drawdown to compute the number of wells extracting each day. Because drawdown is linearly proportional to the rate of extraction in a confined

aquifer, we compute the proportion of the 32 wells in the modeled area that are pumping each day as the ratio of the daily drawdown to the maximum daily drawdown. To account for the variable duration of pumping each day, we perform this calculation with normalized daily drawdowns defined as the daily drawdown divided by the duration of pumping, i.e., a rate of drawdown. Figure 9 confirms that the rate of drawdown is nearly constant over a day, a necessary condition for this normalization. This computed rate of drawdown is shown in Figure 8D. We estimate the maximum daily decline, corresponding to all 32 wells extracting, as the mean daily rate plus one standard deviation, since it is unlikely that the data record contains only one day where all 32 wells are pumping. This assumption in effect implies that all wells were used together 19 days out of the entire 104-day irrigation season. By summing the product of the number of wells pumping on each day, the average pumping rate, and the duration of pumping, and dividing by the irrigated area within the 1.5 km radius (calculated from the IKONIS images Figure 3A to be 65% of the total area), we estimate that 0.72 m of water was applied to the fields during the irrigation season.

We corroborated these results by employing a local farmer to record his schedule of pumping from one irrigation well over the entire season. We determined that the local farmer irrigated his field with a total of 0.9 m of water over the season, a number consistent with the value of 0.72 estimated for our model area, and also consistent with the 1 m of irrigation water for Boro rice cultivation used earlier in our national calculations (Figure 1). However, the proportion of land (~65%) used for irrigated rice in our research area is larger than the national proportion that includes large parts of the country with less or no rice cultivation. The monthly extraction rates are plotted in Figure 3D. Both the extraction rate of this well (~13 L/s) and the area irrigated (~3290 m²) (indicated on map in Figure 3A) are relatively small. Irrigation return flow to the aquifer can be roughly estimated as the water applied to the rice fields minus the water stored in the rice fields and the water lost to evapotranspiration. Given that rice fields are usually irrigated to maintain a standing water depth of ~20 cm [Ali, personal communication], and we estimate evapotranspiration at 28 cm (see below), this return flow is $0.72 \text{ m} - (0.2 \text{ m} + 0.28 \text{ m}) = 0.24 \text{ m}$ for the months of January, February and March. This rough calculation is consistent with previous calculations of irrigation efficiency from the agricultural literature [Yu, 2003] and suggests that irrigation return flow is an important component of the hydrologic system.

5.2.2. Exchange with the River and Ponds

The large head difference between the aquifer and the Ichmatti river (1 to 2 meters, Figure 10) during the dry season demonstrates the potential for significant exchange between the river and aquifer, but also shows that the hydraulic conductivity of the river sediments is much lower than the aquifer conductivity. The sediments in the river channel must severely restrict exchange with the aquifer, however we cannot directly calculate this flux. Because we do not have measurements of the hydraulic conductivity or thickness of these sediments, we cannot directly estimate the exchange between the aquifer and the river. Furthermore, the exchange with the river cannot be estimated from Darcy's law calculations of flux in the aquifer perpendicular to the river because spatial hydraulic gradients within the aquifer are too small to be measured (Figure 10).

The level of the Ichamati river appears to be controlled by the Ganges river even in the dry season when parts of the river become very shallow (<1 m depth). Our measured water levels for the Ichamati river closely follow the water levels recorded by the Bangladesh Water Development Board for the Ganges River at the station in Bhagakul, about 7 km south to our field site (Figure 11), indicating that the Ichamiati is hydraulically connected to the Ganges. Thus, the river level is not a function of local aquifer discharge and recharge, and may be modeled simply as a prescribed head.

Ponds cover ~10% of the land and the majority of these ponds have likely been excavated over the last fifty years as the population has greatly increased. The ponds are excavated to provide clay/silt material for construction of villages above the monsoon flood levels. They receive most of the human waste from the villages and are also used for aquiculture. These ponds do not have a direct connection to the rivers during the dry season. Most are surrounded by clay banks that maintain the water level several meters above both the river stage and the underlying aquifer (Figure 3C). However, water overtops these banks during the flooding season, connecting the ponds to the floodwaters. During the period after flooding and before irrigation, and also the period following irrigation but before the next flood, pond levels are often manipulated for aquiculture by opening and closing canals, so the water levels in the ponds may change dramatically.

During the irrigation season, pond levels drop due to both evaporation and flow to the aquifer. Figure 12 shows this rate of decline computed from heads monitored in eight separate

ponds. All eight ponds lose water at a rate faster than can be explained by evapotranspiration, indicating loss to the aquifer. The average decline for the ponds over the period from January 15, 2004 to April 24, 2004 indicates that ponds contribute about 0.53 mm/day of water to the aquifer, which is about 42% of irrigation pumping.

5.2.3. Rainfall, Evapotranspiration, and Storage Fluxes

Figure 3D shows the average total monthly rainfalls, and one standard deviation, calculated from the last thirty years of data recorded in Bhagakul Meteorological Station, about 4 km southwest to our field site in Munshiganj [WARPO, 2000]. The monthly rainfall for 2003 [BWDB, 2004] is also plotted. Our hydrologic model uses the 2003 monthly hydrologic data, but such data is not yet available for 2004, so we must use averages over the last 30 years for 2004. Fortunately, rainfall is a minor component of the hydrologic system during the first months of the year, the important irrigation period during which the heads decline.

Figure 3D also shows the total monthly reference evapotranspiration for the Munshiganj district averaged over the last thirty years [WARPO, 2000]. These values were calculated from the FAO Penman-Monteith equation [Allen et al., 1998], and vary little from year to year. The reference evapotranspiration, ET_o , was converted into pond evaporation, rice field evapotranspiration, and evapotranspiration from non-irrigated areas using the following factors: $ET_{pan} = \alpha_{pan} ET_o$ ($\alpha_{pan}=1.4$), $ET_{crop} = \alpha_{crop} ET_o$ ($\alpha_{crop}=0.9$), $ET_{tree} = \alpha_{tree} ET_o$ ($\alpha_{tree}=0.95$), where, ET_o , ET_{pan} , ET_{crop} , and ET_{tree} are used for the reference crop, pond water surface, rice and trees, respectively.

Transpiration by trees in villages and along roads (non-irrigated areas) is an important component of the hydrologic system. If trees primarily extract their water from the near-surface clay sediments, they will have little impact on aquifer flow. However, if their roots extend five or six meters (through both the clay mounded to form the village and the underlying overbank-deposit clay) to the much higher yielding aquifer sediments, then transpiration from the trees will be a significant flux of water from the aquifer. ET_{tree} is calculated from ET_o values shown in figure 3D. During the irrigation period of mid-January to late-April, the total value of ET_{tree} is ~40 cm. Since villages cover 22% of the land, this evapotranspiration flux from trees amounts to ~65% of irrigation pumping. We have found no literature specifically describing the root depth of these trees, however many other species are known to extend roots well below 5 meters, and it may be to the advantage of these trees to extract water from below the very low permeability

clay of the villages. However, it is also possible that the roots extract most of their water from the clay. During the dry season, the estimated total ET_{tree} from the villages), ~ 40 cm, can be supplied by the approximately five meters of clay underlying the villages by reducing the water content of the clay by $\sim 8\%$. Since clay is compressible, this would imply that the elevation of villages and roads could rise and fall ~ 40 cm a year! Given this uncertainty, we present modeling results for the two extreme cases where all ET in the non-irrigated areas is extracted from either the near-surface clay or from the aquifer, but find that it makes little difference for other aquifer fluxes.

Water also flows in and out of storage, both from pore-space in the near-surface clays, and in and out of elastic storage in the aquifer. For the model calculations plotted here, the aquifer storativity S was specified at 0.01, corresponding to a specific storage of 10^{-4} m^{-1} over a thickness of 100 m, and the specific yield of the clay was set at 0.02. We choose both of these values to be at the high end of previous estimates [Rahman and Ravenscroft, 2003; Yu et al., 2003], because previous estimates are largely based on pumping tests conducted over durations shorter than the seasonal time scale of our model. Over longer time-scales, the high-storage deep clay that forms the lower confining unit to the aquifer will play a greater role in water storage, and in effect, increase the storage of the aquifer. The specific yield of the surface sediments is only significant in our hypothetical simulations with no pumping, and we also suspect that a large value is appropriate for this parameter because over the long duration of a year more water will drain from a soil. To test the importance of these storage coefficient values, we also conducted several model parameter estimation and simulation runs with $S = 0.001$ and $S_y = 0$, i.e. no storage in the soil.

5.3. Model fitting

We simultaneously solved the equations for the lumped-parameter model numerically with the Matlab function *ODE45*, and embed this numerical solution into Matlab's *lsqnonlin.m* least squares algorithm to estimate the four conductances by minimizing the sum of square differences between the measured and modeled heads. The terms of the sum of square errors are:

$$SSE = \sum_i^{n_a} \left(h_{a,i} - \bar{h}_{a,i} \right)^2 + \sum_i^{n_v} \left(h_{v,i} - \bar{h}_{v,i} \right)^2 + \sum_i^{n_f} \left(h_{f,i} - \bar{h}_{f,i} \right)^2 + \sum_i^{n_p} \left(h_{p,i} - \bar{h}_{p,i} \right)^2 \quad (5)$$

where n_a, n_v, n_f, n_p , are the number of head observations in (respectively) the aquifer, the clays in the non-irrigated villages and roads, the clays in the field and the ponds, $h_{a,i}, h_{v,i}, h_{f,i}, h_{p,i}$, are the observed heads in the aquifer, non-irrigated areas, fields and ponds, and $h_{a,i}^m, h_{v,i}^m, h_{f,i}^m, h_{p,i}^m$, are the modeled heads in the aquifer, non-irrigated areas, fields and ponds. We assessed the quality of the parameter fits from the sum of square errors by computing the parameter covariance matrix as the Cramer-Rao lower bound [Milton and Arnold, 1995] using the Matlab function `n4sid`. The covariance matrix provides information about parameter uncertainty and correlation. The diagonal provides the variance of the parameter estimates and the off-diagonal terms indicate the covariance of the estimates. If parameters are highly correlated, then they cannot be independently estimated with reliability, suggesting that more data is required or that the model is incorrectly structured.

5.4. Model Results

The fitted conductances and their estimated uncertainties, Tables 1, 2 and 3, suggest that the simple lumped parameter model may accurately represent the basic behavior of the true system. First, the modeled heads closely fit the observed heads and water levels (Figure 13). Second, the estimated parameter uncertainties are low as evidenced by their small coefficients of variation, and they are not strongly correlated, suggesting that the model is not over parameterized. Third, the estimated values for all four conductances (table 1) are typical for these types of clay or silty sediments [Freeze and Cherry, 1979].

Because we do not know the depth of tree roots, we fit conductances for the two extreme cases where transpiration is drawn up by roots either in the near-surface clay only, or in the underlying aquifer only. As we describe later, both approaches lead to the same conclusions about the role of hydrology on arsenic behavior.

The conductance estimates are in accord with expectations for interface sediments between the aquifer and various reservoirs. To compute the hydraulic conductivity of these interface sediments, we must multiply the conductance by the thickness of the unit in the direction of flow. For the river-aquifer interface, with an assumed 2 m thick interface unit, the hydraulic conductivity is 1.8×10^{-6} m/s, and 2.0×10^{-6} m/s for the case where transpiration from trees is drawn from the clay and aquifer, respectively. This corresponds to a silty-clay. Similarly, assuming a 1m thick unit at the bottom of the pond, a 2 m thick unit for the fields and a 6 m thick

unit for the non-irrigated villages and roads yields hydraulic conductivities for the pond of 1.0×10^{-7} m/s and 9.6×10^{-8} m/s, for the fields of 2.0×10^{-8} m/s and 2.0×10^{-8} m/s and for the non-irrigated areas of 4.4×10^{-10} m/s and 6.3×10^{-8} m/s, where the two figures correspond to cases where tree transpiration is drawn from the clay and aquifer, respectively.

The coefficient of variation of the estimated parameters is well below 20% for all the conductances except for the conductance of non-irrigated areas when the ET is taken from the non-irrigated clay and with specified storage parameters. In this case, the coefficient of variation is ~550% indicating that the modeled heads are insensitive to this parameter. When the ET is taken from the clay, there is very little flow from non-irrigated areas to the aquifer and the heads in the non-irrigated areas agree well with the data (Figure 13A). Thus, for this case, the conductance of the clay in the non-irrigated areas does not influence the modeled heads significantly and so cannot be estimated accurately. These sediments contribute a relatively small component of the hydrologic cycle and the model is therefore relatively insensitive to this parameter, as indicated by the large coefficient of variation.

We fixed the value of the two storage parameters, the specific yield of the clay ($S_y = 0.2$) and the storativity of the aquifer ($S = 0.01$) because neither of these parameters can be reliably estimated from available data. Also, the values assigned to these parameters have little impact on our results. The specific yield of the clay underlying the rice fields has little impact during irrigation because water is ponded above the clay, and accordingly these areas are given a storage parameter value of 1 during ponding in the model. The specific yield of the village clay also has little impact because: (1) in the case where transpiration is extracted from the clay, there is essentially no flow to the aquifer, and; (2) in the case where trees draw water from the aquifer, the specific yield cannot be estimated independently of the conductance of the clay (S_y and k_v are highly correlated, Table 3) since increasing either parameter will increase the flux to the aquifer. Furthermore, the specific yield of the clay has little impact on predicted flows in the absence of irrigation because the rice fields yield little water to aquifer (Figure 14).

The storativity of the aquifer cannot be estimated accurately because the estimated value is strongly correlated to the estimated conductance of the river. Including aquifer storativity in the parameter estimation procedure results in a correlation coefficient of 0.81 for S and k_r (Table 3). The parameters are linked because they affect the modeled heads in the same way: in the first half of the dry season, as heads are falling, increasing either the model aquifer storage or the

river conductivity will decrease the rate of head decline; likewise, during the latter period as heads are rising, increasing either parameter will decrease the rate of head rise. Thus, if the aquifer storage is much lower than 0.01, the flux in and out of the river will be decreased by the same amount as the decrease of flux in and out of storage. This flux is relatively small (Figure 14), so the calculated residence times will only slightly increase for current conditions, but the effect on residence times is more significant in the absence of pumping because other fluxes are smaller. Without pumping, model results for $S=0.001$ and $S_y = 0$ (no soil flux) indicate the groundwater residence time may be increased to over 120 years (not shown).

5.5. Recharge and Discharge Fluxes and Their implications for Arsenic

The model was used to examine water residence times as well as fluxes between the various reservoirs, with and without irrigation pumping. The net yearly flux into or out of the aquifer, shown in Figure 14, can be used to compute water residence times within the aquifer by dividing the aquifer volume by the yearly flux. These residence times, Table 1, show that for the pumping scenario the residence time is 26 and 38 years, respectively for the two ET cases, and without pumping, residence times are 44 and 84 years, respectively (assuming the presence of the modern number of ponds). These residence times are consistent with the bomb-levels of tritium and carbon-14 measured to a depth of 30 m. An important conclusion can be immediately drawn from the analysis – the flushing time of the aquifer, with or without pumping, is rapid compared to the age of the basin. Accordingly, the recent introduction of large-scale pumping itself may not solely explain why arsenic has not been flushed from the aquifer long ago. As we discuss next, pumping does, however, change the hydrologic balance and water sources to the aquifer, which likely has major implications for arsenic dynamics. It should also be remembered that the residence time is not the same as the average groundwater age; a low residence time may imply rapid flow at only very shallow depths with stagnant water below. The lumped-parameter model does not distinguish flow rates at different depths.

Figure 13 shows the estimated water fluxes (volume flux per total land area in mm/day) as a function of time, for the two different ET cases: with and without pumping. The line labeled “storage” shows the net rate of water release from (positive) or replenishment to the aquifer (negative), which must balance the sum of all the other fluxes at each instant.

We first discuss the current situation with pumping. For the ET from clay case, the model predicts that during pumping, water initially leaves the aquifer to the river, but then the fluxes

reverse, and the river becomes a source of water to the aquifer. Water is released from storage in the aquifer at the onset of pumping, and is returned to storage at the cessation of the pumping season. During most of the irrigation season, the aquifer is neither releasing nor taking significant water from storage, but is acting as a flow-through reservoir. Water mainly leaves the aquifer by pumping, and enters at roughly equal rates from the irrigated fields and ponds and, in the later half of the irrigation season, from rivers. There is very little flux to or from the non-irrigated village areas. The water balance for the case where tree transpiration is taken directly from the aquifer appears roughly the same as for the case of tree transpiration loss from the non-irrigated clays, except that the transpiration loss from the aquifer, which is only slightly smaller than the pond and field flux, is approximately balanced by a leakage flux from the non-irrigated areas. In summary, with pumping, water principally leaves the aquifer by pumping, and to a lesser degree is initially lost to the river. Water principally enters the aquifer from the irrigated fields and ponds, and later in the season from the river. Because the aquifer is semi-confined, and because there is little rainfall during the irrigation season, direct rainfall is a minor component of aquifer recharge. The ET and leakage from the non-irrigated village areas balance each other out.

While the vigor of the aquifer circulation is reduced in the non-pumping scenario, the more important observation may be that water balance shifts. Again, transpiration and leakage from the village areas (non-irrigated) more or less balance. Water principally leaves through the river over most of the year, but water fluxes from the ponds are approximately two times greater than fluxes from the fields. The fluxes from the fields are reduced by two compounding effects. First, the fields are no longer flooded in the non-pumping scenario, so there is no ponded water to drive water down into the aquifer. Second, the downward gradient into the aquifer is less without pumping, because the hydraulic head in the aquifer is not drawn down. The large source of water from the ponds does not necessarily represent pre-irrigation conditions, because many of the ponds likely did not exist more than 50 years ago. If the ponds are removed from the model to represent past conditions, then the estimated flux through the system is greatly reduced. Consequentially, the groundwater residence times may have been much greater in the past when there were many fewer excavated ponds.

The hydrologic balances computed above for pumping and non-pumping suggest that the ponds and flooded rice fields are likely recent sources of anaerobic, organic-rich recharge waters.

Indeed, widespread flooding during the dry season coupled with pumping would both promote anaerobic conditions and provide the gradients necessary to drive water into the aquifer. In the absence of pumping, the flux of water from the fields is reduced by half but more importantly would likely be much less reducing in the absence of flooding and rice cultivation. In contrast, wide-spread flooding during the monsoon causes little infiltration of reducing bottom water because heads in the aquifer, rivers and fields equilibrate. Because the aquifer is semi-confined, heads rise quickly after irrigation ceases from the input of relatively small amounts of surface water. Thus, pumping-induced shifts in the hydrology of Bangladesh coupled with population growth, rice cultivation and excavation of ponds may be creating large perturbations in the subsurface biogeochemistry of Bangladesh.

6. Conclusion

Arsenic concentrations in groundwater in Bangladesh vary greatly over short distances; water with dangerously high levels is found in wells that are tens of meters from wells with safe water. Undoubtedly some of this variation is caused by differences in bulk sediment composition, such as variations in the sorption capacity of grey sediment and orange/brown sediment that contains more oxides. However, large gradients in arsenic concentrations are found within grey aquifer sediment where there is little difference in the solid characteristics and many drinking water wells extract groundwater. At our study site in Munshiganj, a wide variety of data support the hypothesis that the pattern of groundwater arsenic concentrations is related to the pattern of groundwater flow. Where the mineral composition of aquifer material is homogeneous, the most likely explanation for large differences in groundwater arsenic concentration is that concentrations are related to the flow path of the groundwater. Some flow paths, such as fast paths terminating in irrigation wells, may flush arsenic from the system, and may now have low arsenic concentrations. Other flow paths may introduce oxidants that immobilize dissolved arsenic and hence contain relatively low concentrations. Yet other flow paths may have high arsenic concentrations because they originate from areas where reductive processes are mobilizing arsenic. Such a flow path is evident at 30 m depth at our field site where arsenic and the products of organic carbon oxidation are strongly correlated. Because areas of recharge (rice fields, ponds, river channels) and discharge (irrigation wells, river

channels) are spaced tens and hundreds of meters apart, the chemical heterogeneity caused by different flow paths will be similarly spaced.

Groundwater irrigation has greatly changed the location, timing and chemical content of recharge to the aquifer. During the dry season, irrigation water is ponded in rice fields over approximately half of our total research site, thereby changing both the hydrologic budget and the biogeochemistry of recharge water. Irrigation enhances recharge by both lowering the head in the aquifer beneath the near-surface clay, and by raising the head above the clay. The resulting return flow to the aquifer is anoxic and probably rich in organic matter, potentially driving reduction of oxides that may be present in the near surface sediments, or deeper in the aquifer. This process does not repeat during the flood season. When the land is inundated during the monsoon, near surface sediment porewater may become anoxic, but recharge ceases because there is no driving potential gradient in the water column. Permanent constructed surface water bodies, primarily ponds excavated near villages, also provide a large source of recharge to the aquifer. Because these ponds receive the waste from nearby villages, they are a potential source of organic carbon to the subsurface, and because they are located near the drinking water wells in these villages, they may affect the groundwater withdrawn by these wells.

The hydrologic data and modeling from our site indicate that groundwater flow is vigorous, flushing the aquifer over time-scales of decades but also rapidly transporting a solute load into the aquifer with recharge water from rice fields, ponds and rivers. The net effect is certainly a complex transient three-dimensional pattern of groundwater flow paths with differing solute concentrations. Fully understanding the spatial and temporal patterns of dissolved arsenic concentrations will require detailed distributed-parameter hydrogeologic models that describe how groundwater carries solutes into the subsurface, and flushes solutes from the subsurface. Constructing such models will require the level of hydrogeologic characterization that is employed at groundwater contamination sites in North America and Europe. Only with such characterization and modeling will we address broad questions such as whether arsenic concentrations will generally rise or fall over time, or whether dissolved arsenic will penetrate deeper into aquifers in the future. The combined hydrologic and biogeochemical results presented here imply that the system may not be in steady-state and that the net effect of competing processes could either increase or decrease arsenic concentrations over the next decades.

Acknowledgements – We thank three anonymous reviewers for their very helpful suggestions.

This work was funded by the National Science Foundation (Grant number EAR-0001098).

References

- 1 Abedin, M.J., Cotter-Howells, J., Meharg, A.A., 2002. Arsenic uptake and accumulation in rice (*Oryza sativa* L.) irrigated with contaminated water. *Plant and Soil*, 240(2), 311-319.
- 2 Aggarwal, P.K, Basu, A.R., Poreda, R.J., 2002. Isotope hydrology of groundwater in Bangladesh: Implications for characterization and mitigation of arsenic in groundwater. IAEA-TC Project Report: BGD/8/016, IAEA, Vienna.
- 3 Aggarwal, P.K, Basu, A.R., Kulkarni, K.M., 2003. Comment on “Arsenic mobility and groundwater extraction in Bangladesh” (I). *Science*, 300(5619).
- 4 Allen, R.G., Pereira, L. S., Raes, D., Smith, M., 1998. Crop evapotranspiration - Guidelines for computing crop water requirements - FAO Irrigation and drainage paper 56. FAO - Food and Agriculture Organization of the United Nations Rome, M-56, ISBN 92-5-104219-5
- 5 Ali, M. A., 2003. Fate of Arsenic in the Environment, *Arsenic Contamination: Bangladesh Perspective*, edited by M. F. Ahmed, ITN-Bangladesh.
- 6 Appelo, C.A.J., Van der Weiden, M.J.J., Tournassat, C., Charlet, L., 2002. Surface complexation of ferrous iron and carbonate on ferrihydrite and the mobilization of arsenic. *Environmental Science and Technology*, 36(14), 3096-3103.
- 7 BADC, 2003. Survey Report on Irrigation Equipment and Irrigated Area in Boro/2003 Season, Bangladesh Agricultural Development Corporation.
- 8 BADC, 2002. Survey Report on Irrigation Equipment and Irrigated Area in Boro/2002 Season, Bangladesh Agricultural Development Corporation.
- 9 Bangladesh Water Development Board (BWDB), 2004. Surface water and rainfall data for Bhagakul Meteorological Station, Munshiganj (personal communication).
- 10 BGS and DPHE, 2001. Arsenic Contamination of Groundwater in Bangladesh. Kinniburgh, D.G. and Smedley, P.L. (editors). Volume 1-4, British Geologic Survey Report WC/00/19, (<http://www.bgs.ac.uk/arsenic/Bangladesh>).
- 11 Brammer, H, and Brinkman, R., 1977. Surface-water Gley Soils in Bangladesh: Environment, Landforms and Soil Morphology. *Geoderma*, 17, 91-109
- 12 Brammer, H., 1996. *The Geography of the Soils of Bangladesh*. University Press Limited, Dhaka, Bangladesh, ISBN 984 05 1328.

- 13 Breit G., Foster, A. L., Whitney J. W., Uddin N. Md., Yount, J. C., Welch A. H., Alam M. Md., Islam S. Md., Sutton S., and Newville, M., 2001. Variable arsenic residence in sediment from eastern Bangladesh: clues to understanding arsenic cycling in the Bengal delta. Abstract presented at International Conference on Arsenic in Drinking Water, hosted by Columbia University Superfund Basic Research Program, Columbia University, November, 2001.
- 14 Brinkman, R., 1977. Surface-water Gley Soil in Bangladesh: Genesis. *Geoderma*, 17, 111-144.
- 11 Dixit, S., Herring, J.G., 2003. Comparison of arsenic(V) and arsenic(III) sorption onto iron oxide minerals: Implications for arsenic mobility. *Environmental Science and Technology*, 37(18), 4182-4189.
- 12 Freeze, R.A. and Cherry, J.A., 1979. *Groundwater*. Prentice-Hall, Upper Saddle River, NJ.
- 13 Freeze, R. A., Witherspoon, P. A., 1966. Theoretical analysis of regional groundwater flow: 1. Analytical and numerical solutions to the mathematical model. *Water Resources Research*, 3, 623-634.
- 14 Harvey, C.F., Swartz, C.H., Badruzzman, A.B.M., Keon-Blute, N., Yu, W., Ali, M.A., Jay, J., Beckie, R., Niedan, V., Brabander, D., Oates, P.M., Ashfaque, K.N., Islam, S., Hemond, H.F., Ahmed, M.F., 2002. Arsenic mobility and groundwater extraction in Bangladesh. *Science*, 298, 1602-1606.
- 15 Harvey, C.F., Swartz, C., Badruzzman, A.B.M., Keon-Blute, N., Yu, W., Ali, M.A., Jay, J., Beckie, R., Niedan, V., Brabander, D., Oates, P., Ashfaque, K., Islam, S., Hemond, H., Ahmed, M.F., 2003. Response to Comments on "Arsenic Mobility and Groundwater Extraction in Bangladesh," *Science*, 300(5619).
- 16 Hossain, M., Lewis, D., Bose, M. Chowdhury, A., 2003. Rice research: Technological progress and impacts on the poor: The Bangladesh case (Summary Report), International Food Policy Research Institute (IFPRI).
- 17 Islam, F. S., Gault, A., Boothman, C., Polya, D., Charnock, J., Chatterjee, D., Lloyd, J., 2004. Role of metal-reducing bacteria in arsenic release from Bengal delta sediments, *Nature*, 430, 68-71.
- 18 Kinniburgh, D.G., Smedley, P.L., Davies, J., Milne, C.J., Gaus, I., Trafford, J.M., Burden, S., Huq, S.M.I., Ahmad, N., Ahmad, M.K., 2003. The scale and causes of the groundwater arsenic problem in Bangladesh. *Arsenic in Ground Water: Geochemistry and Occurrence*

- (eds. A.H. Welch and K.G. Stollenwerk). Kluwer Academic Publishers, Boston, MA, pp. 211-257.
- 19 McArthur, J.M., Banerjee, D.M., Hudson-Edwards, K.A., Mishra, R., Purohit, R., Ravenscroft, P., Cronin, A., Howarth, R.J., Chatterjee, A., Talukder, T., Lowry, D., Houghton, S., Chadha, D.K., 2004. Natural organic matter in sedimentary basins and its relation to arsenic in anoxic ground water: the example of West Bengal and its worldwide implications. *Applied Geochemistry*, 19(8), 1255-1293.
 - 20 Meharg, A.A., Rahman, M., 2003. Arsenic contamination of Bangladesh paddy field soils: Implications for rice contribution to arsenic consumption. *Environmental Science and Technology*. 37(2), 229-234.
 - 21 Milton, J.S., Arnold, J.C., 1995. *Introduction to Probability and Statistics: Principles and Applications for Engineering and the Computing Sciences*, McGraw-Hill, New York.
 - 22 MoA 2004, *Handbook of Agricultural Statistics*, Sector Monitoring Unit, Ministry of Agriculture.
 - 23 Nickson, R., McArthur, J., Burgess, W., Ahmed, K.M., Ravenscroft, P., Rahman, M., 1998. Arsenic poisoning of Bangladesh groundwater. *Nature*, 395, 338.
 - 24 Oremland, R. S., and Stolz, J. F., 2005, Arsenic, microbes and contaminated aquifers, *Trends in Microbiology*, 13(2).
 - 25 Polizzotto, M.L., Harvey, C.F., Li, G., Newville, M., Fendorf, S., 2004. Solid-Phases and Desorption Processes of Arsenic within Bangladesh Sediments, *Chemical Geology*, in press.
 - 26 Rahman, A.A., Ravenscroft, P., eds., 2003. *Groundwater Resources and Development in Bangladesh*, The University Press Ltd, Dhaka Bangladesh, ISBN 984 05 1643 4
 - 27 Shankar, B., Halls, A., Barr, J., 2004. The Effects of Surface Water Abstraction for Rice Irrigation on Floodplain Fish Production in Bangladesh. *International Journal of Water*. (accepted).
 - 28 Swartz, C.H., Keon, N.E., Badruzzaman, B., Ali, A., Brabander, D., Jay, J., Islam, S., Hemond, H.F., Harvey, C.F., 2004. *Subsurface Geochemistry And Arsenic Mobility In Bangladesh*. *Geochemica Acta*, in press.
 - 29 van Geen, A., Zeng, Y., Versteeg, R., Stute, M., Horneman, A., Dhar, R., Steckler, M., Gelman, A., Small, C., Ahsan, H., Graziano, J., Hussein, I., Ahmed, K., 2003. Spatial variability of arsenic in 6000 tube wells in a 25 km² area of Bangladesh. *Water Resources*

Research, 39(5), 1140.

- 30 van Ranst, E., and de Coninck, F., 2002. Evaluation of ferrollysis in soil formation. *European Journal of Soil Science*, 53, 513-51
- 31 Water Resources Planning Organization (WARPO), 2000. National Water Management Plan Project: Draft Development Strategy. Ministry of Water Resources, Government of the People's Republic of Bangladesh.
- 32 Yu, W.H., Harvey, C.M., Harvey, C.F., 2003. Arsenic in the groundwater in Bangladesh: A geostatistical and epidemiological framework for evaluating health effects and potential remedies. *Water Resources Research*, 39(6), 1146.
- 33 Yu, W., 2003. Socio-Hydrologic approaches for managing groundwater contamination problems: strategies for the arsenic problem in Bangladesh. Doctoral thesis, Division of Engineering and Applied Sciences, Harvard University, Cambridge, MA, USA.

Figure Captions

Fig.1 (A) Cultivation of high-yielding bororice has greatly expanded since 1970 to cover approximately 20% of Bangladesh, or approximately 45% of the cultivatable area. Most boro is irrigated by groundwater so extraction has also risen. Data taken from Hossain et al [2003]. (B) Yearly maximum depth to groundwater in wells between 1988 and 1997 (data source: WARPO, 2000). The filled and unfilled symbols represent the average yearly maximum depths in six geographic regions of Bangladesh: the north and south, divided into east, central and west sections. The solid line represents the country average of yearly maximum depths. Error bars represent the standard error of the mean (standard deviation divided by square root of n-1). The country average, as well as all the hydrologic regions, have a pattern of increasing maximum depths.

Fig.2 Concentrations of sulfate, arsenic, calcium and ammonium from the Munshiganj field site [Harvey et al, 2002] compared to the BGS and DPHE [2001] national data set. The median, mean and 90th percentile are plotted for the BGS data for a bin size of ~200 data points. Using a constant bin size causes unequal depth intervals; intervals are small where many wells are screened at ~25 m depth.

Fig.3 (A) IKONOS satellite image of 16km² study area in Munshiganj with hydrologic monitoring locations at irrigation wells, drinking wells, ponds and bridges over the Ichhamati river channels. The rice field where irrigation was monitored is also shown. (B) Center section of the study area highlighting the Ichhamati river main channel, side channel, and intensive field site near the center. (C) Water levels within the Munshiganj study area shown in Figure 3B between March 2003 and July 2004. The flooding season extends from June to October with the flood peak in August, and dry season irrigation extends from January to April with a groundwater minimum in March. Repeated surveys of well casing and benchmark elevations by theodolite indicated that level errors were less than 1 cm. (D) Monthly rainfall, evapotranspiration (ET), and irrigation data. Both the monthly average (for last 30 years prior to 2002 [WARPO, 2000]) and 2003 rainfall [BWDB, 2004] were measured at the meteorological station in Bhagakul, about 4 km

southwest of our field site. ET was calculated from data measured in Munshiganj district [WARPO, 2000]). The irrigation water applied to a monitoring rice field in our study area (Figure 3A) during the 2003-2004 irrigation season is also shown.

Fig.4 (A) Horizontal hydraulic conductivity as estimated from pumping tests [Yu, 2003] at the intensive study site Figure 3B. The conductivity at 22 m is uncertain because of well silting, but appears to be lower than at other depths. (B) Hydraulic heads relative to the 20 m piezometer during the dry season, early irrigation (January) and late irrigation (May). The inset represents heads in May measured with a manometer that obtains relative differences to within 1 mm. (C) Oxygen-18 isotope ratios relative to SMOW. The convergence of vertical flow at 38 m in May is below the low conductivity at 22 m, but is not consistent throughout the year, as evidenced by the January data. These data are all local to our small intensive study site.

Fig.5 (A) Plot of daily groundwater level (as recorded by In-Situ Mini-Troll© pressure transducer, automatically corrected for barometric changes) at Munshiganj field site over the last three years from a 30 m well. Transducer data was not collected during the winter/spring of 2003, so manual water level dipping data are shown. In other years, the results of manual dipping were indistinguishable from transducer data. The plot also shows the difference in water level between the shallow and deep (from 165 m well) aquifer. (B) Plot of hourly groundwater highlighting the transition to irrigation season in early January of two separate years. During the irrigation period, heads oscillate by about 20 cm as irrigation pumps are turned off and on. The small oscillations before and after the pumping season are consistent with barometric oscillations expected for a confined aquifer.

Fig.6 Schematic diagram of the lumped-parameter model highlighting different recharge and discharge fluxes along with the parameter and variables used in for the numerical model.

Fig.7 Distribution of measured pumping rates of 41 irrigation wells within the Munshiganj study area. The mean and median of the distribution is 24.1 L/s and 25.0 L/s, respectively. Rates were measured directly by recording the time to fill known volume.

Fig.8 (A) Aquifer head data for a 30 m well at the intensive filed site for the period of December 2003 to July 2004 as shown in Figure 5A. (B) Daily fluctuations in groundwater head, calculated by subtracting a 24-hour moving average from the raw head data presented in panel (A). (C) Calculated pumping duration for the 2003-2004 irrigation season. (D) Rate of daily aquifer drawdown, calculated by dividing the amplitude of head oscillations by the pumping duration for each day. Data is used to scale the number of wells pumping on each day.

Fig.9 Head data and exponential curve fit for: (i) Five days in January with a 10-hr pumping duration, (ii) Five days in February with an 11-hr pumping duration, (iii) 100 consecutive days beginning January 7, 2002, with variable pumping duration. The data on each day was normalized to zero at the maximum, then averaged on each subsequent hour of pumping, ending at the minimum head value, or end of pumping. The fits show that the rate of decline increases from January to February, and that the rate is approximately linear with time. However, the data also show an unexplained inflection from concave to convex.

Fig.10 River stage of the Ichhamati River (also in Figure 3C) and hydraulic head measured in nearby wells (mapped in Fig.4B) during December 2003 to July 2004. The error bars (of 20 cm) associated with the groundwater levels (from January to April) account for the water level fluctuation due to irrigation pumping (Fig. 5B). The groundwater heads are located along a transect roughly perpendicular to the river, but show no appreciable hydraulic gradient even though the river head differs from the aquifer head by more than a meter.

Fig.11 Comparison between Ganges water level (as recorded in Bhagakul Meteorological Station [BWDB, 2004]) and Ichhamati water level (within the study area). The water

levels follow each other closely. The pink squares represent the average of both the main channel and side channel (Figure 3) that we used to fit the model, whereas the green triangles represent the water levels in the main channel only. The oscillations in the Ganges water level at a 14-day frequency are likely the effect of aliasing with tides: Measurements are taken twice every day at the same time, so tidal oscillations in the Ganges appear as cycles with 14 day frequencies. The groundwater heads at our site (Figure 8) do not show any evidence of tides.

Fig.12 The rate of pond water level (PWL) decline for 7 ponds (mapped in Figure 3A), and the rate of pan evaporation (ET) and rainfall (RF) for the period of Dec 2003 to April 2004. Rates of PWL decline were calculated by dividing the difference in PWLs by the duration between the two measurements. Positive differences indicate a decline.

Fig.13 (A) Model fits and predictions for the case where transpiration from the villages (trees) is extracted from the village clay. The first panel (upper-left) shows the best model fit to the data, with the corresponding model fluxes in and out of the aquifer system plotted below. The pumping flux is prescribed. The upper-right panel shows the predicted heads in the absence of pumping and irrigation, with the corresponding fluxes plotted below. **(B)** The same set of plots as in **A**, except here the transpiration of the villages is modeled as coming from the aquifer (i.e. tree roots are all modeled as extending through the village clay). The model results differ because they now show significant ET from the aquifer and a roughly corresponding increase in recharge to the aquifer from the village clay.

Fig.14 The estimated (with pumping) and predicted (without pumping) annual water fluxes into and out of the aquifer, for the case where transpiration from the village trees is extracted from the clay **(A)** and from the underlying aquifer **(B)**. These yearly fluxes are calculated by integrating the instantaneous fluxes shown in Figure 13 over time.

Tables

Table 1. The estimated conductance parameter values when the storage coefficients are fixed, the respective objective functions (sum of square errors), and modeled residence times for the aquifer.

Table 2. The correlation coefficients and the coefficient of variation (CV) of estimated parameters when the four conductance parameters are estimated simultaneously. Both the cases where ET from the village trees is withdrawn from village clay and from the underlying aquifer are given.

Table 3. The correlation coefficients and the coefficient of variation (CV) of estimated parameters when the four conductance parameters and the two storage parameters are all estimated simultaneously. Both the cases where ET from the village trees is withdrawn from village clay and from the underlying aquifer are given.

Tables

		Case-A	Case-B
Village ET_{tree} from		Clay	Aquifer
k_f (1/d) [conductance for field]		8.9×10^{-4}	8.9×10^{-4}
k_v (1/d) [conductance for village]		6.3×10^{-6}	9.1×10^{-4}
k_p (1/d) [conductance for pond]		9.3×10^{-3}	8.3×10^{-3}
k_r (1/d) [conductance for river]		7.7×10^{-2}	8.7×10^{-2}
Objective Function <i>w/ pumping</i>		5.9×10^{-1}	5.7×10^{-1}
Residence Time (yrs)	<i>w/ pumping</i>	38	26
	<i>w/o pumping</i>	84	44

Case A: Village ET out of Clay						
	k_f	k_p	k_r	k_v		CV
k_f	1					0.11
k_p	-0.18	1				0.10
k_r	-0.28	0.29	1			0.11
k_v	-0.30	0.01	0.09	1		5.45
Case B: Village ET out of Aquifer						
	k_f	k_p	k_r	k_v		CV
k_f	1					0.10
k_p	-0.21	1				0.10
k_r	-0.31	0.23	1			0.10
k_v	-0.11	0.05	0.00	1		0.06

Case A: Village ET out of Clay							
	k_f	k_p	k_r	k_v	S_y	S	CV
k_f	1						0.15
k_p	-0.17	1					0.09
k_r	-0.31	0.04	1				0.10
k_v	-0.34	0.02	-0.22	1			0.77
S_y	-0.26	0.02	-0.29	0.92	1		0.14
S	-0.24	-0.07	0.81	-0.15	-0.19	1	0.13
Case B: Village ET out of Aquifer							
	k_f	k_p	k_r	k_v	S_y	S	CV
k_f	1						0.18
k_p	-0.11	1					0.09
k_r	-0.39	-0.06	1				0.11
k_v	-0.36	0.10	-0.07	1			0.08
S_y	-0.36	0.11	-0.10	0.79	1		0.09
S	-0.26	-0.14	0.83	-0.16	-0.22	1	0.15

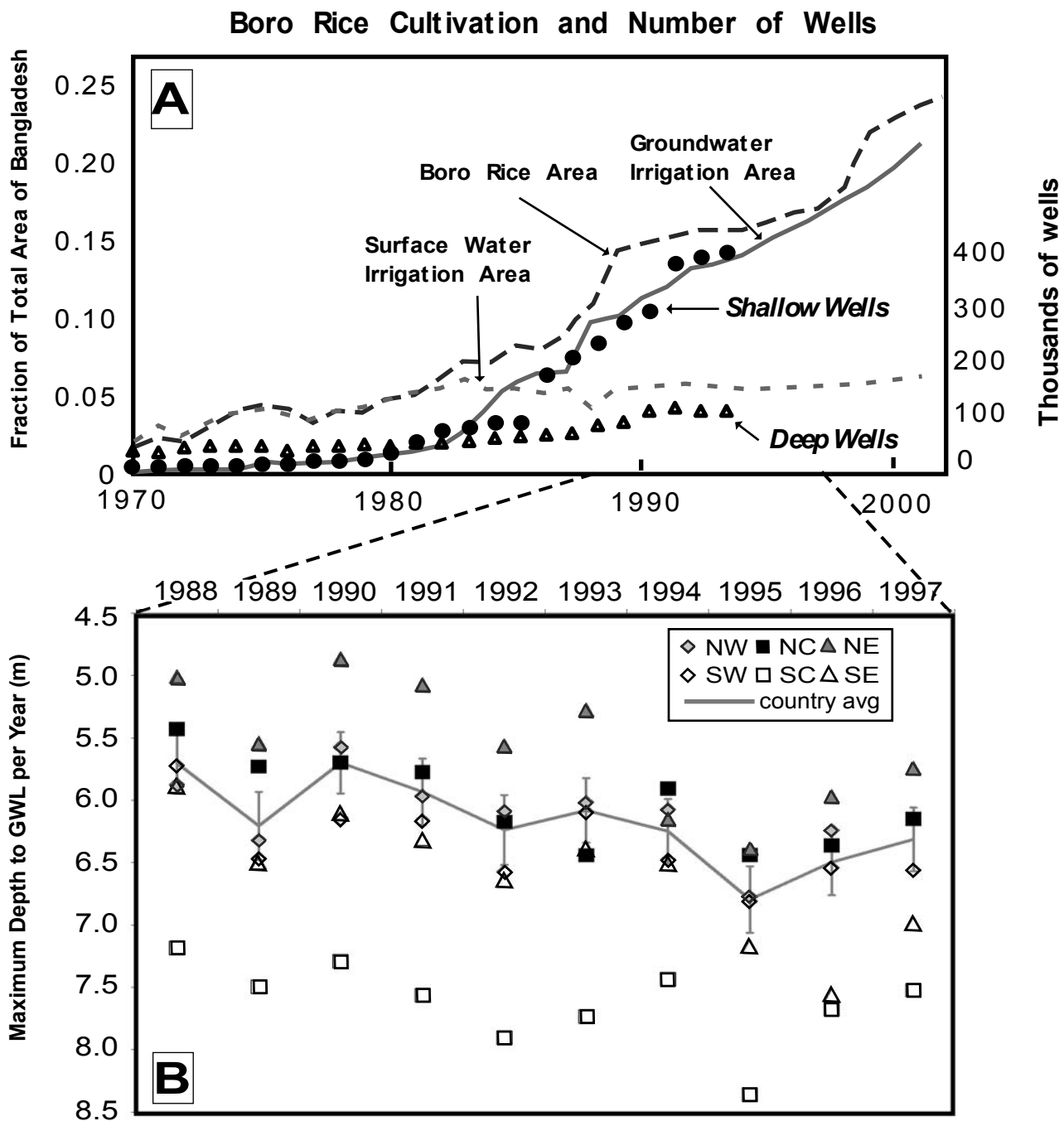


Fig.1

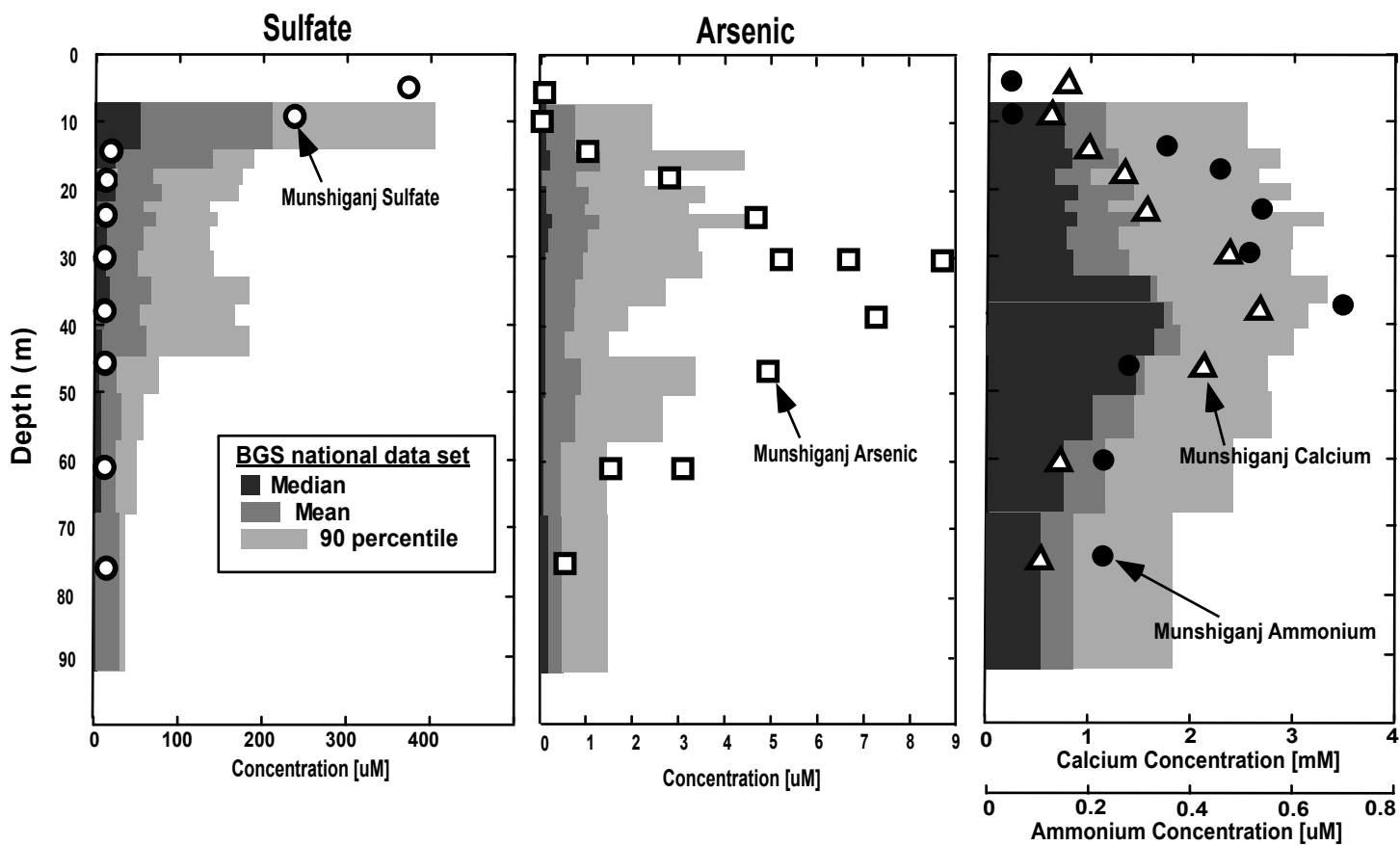


Fig.2

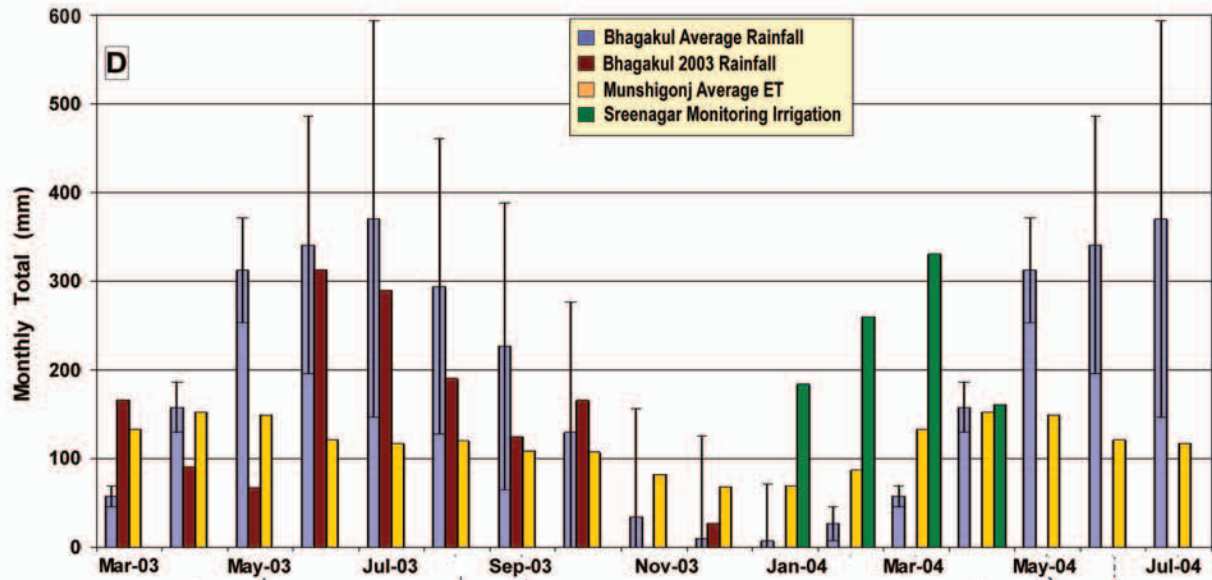
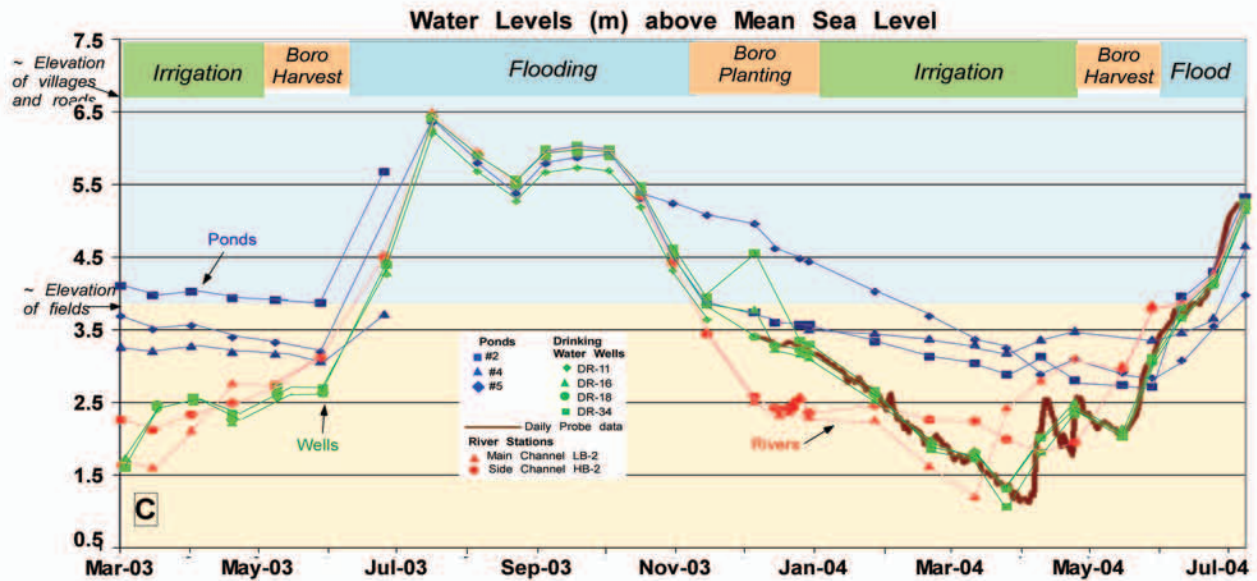
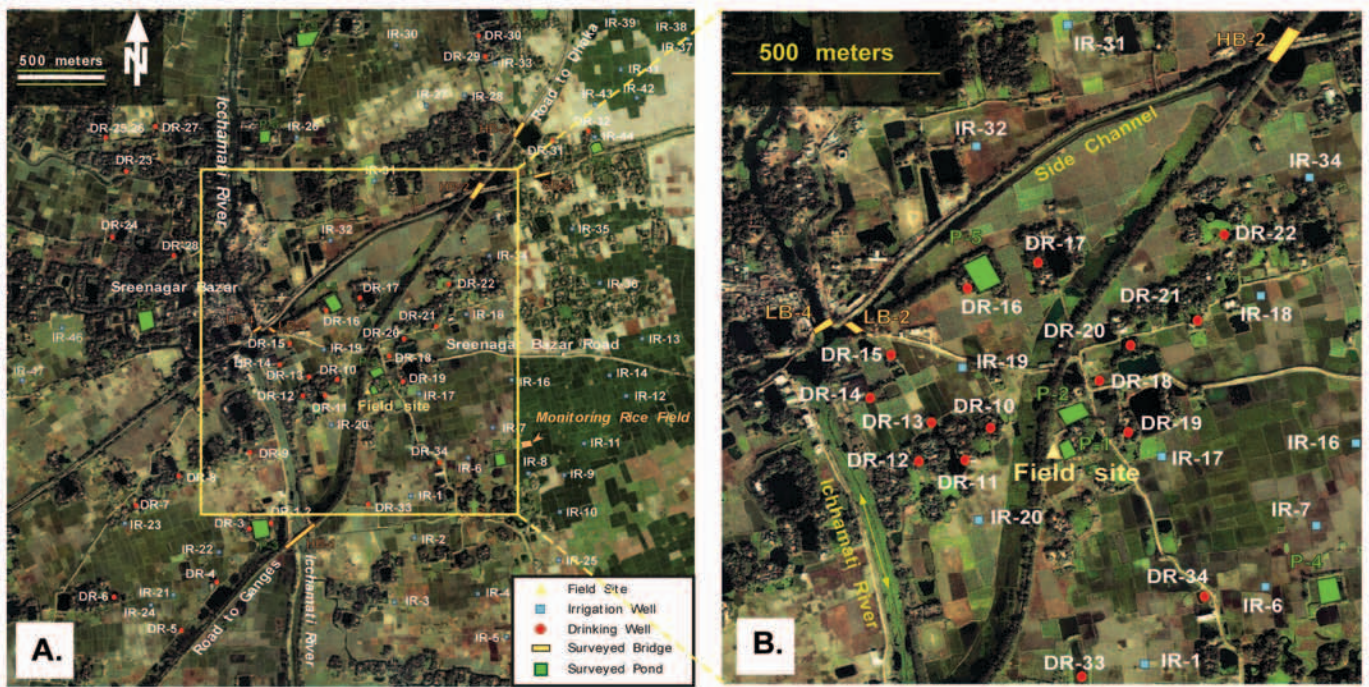


Fig.3

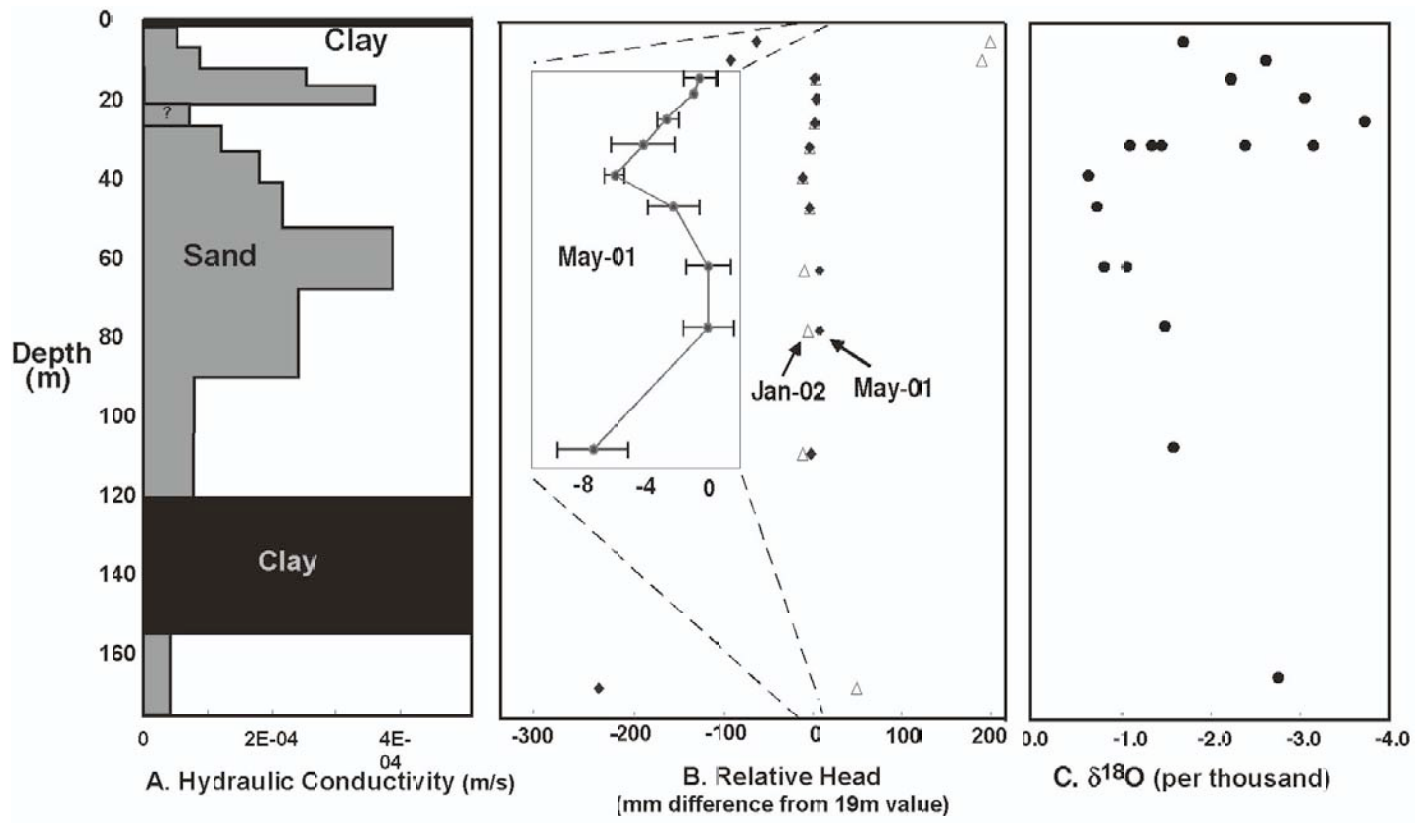


Figure 4.

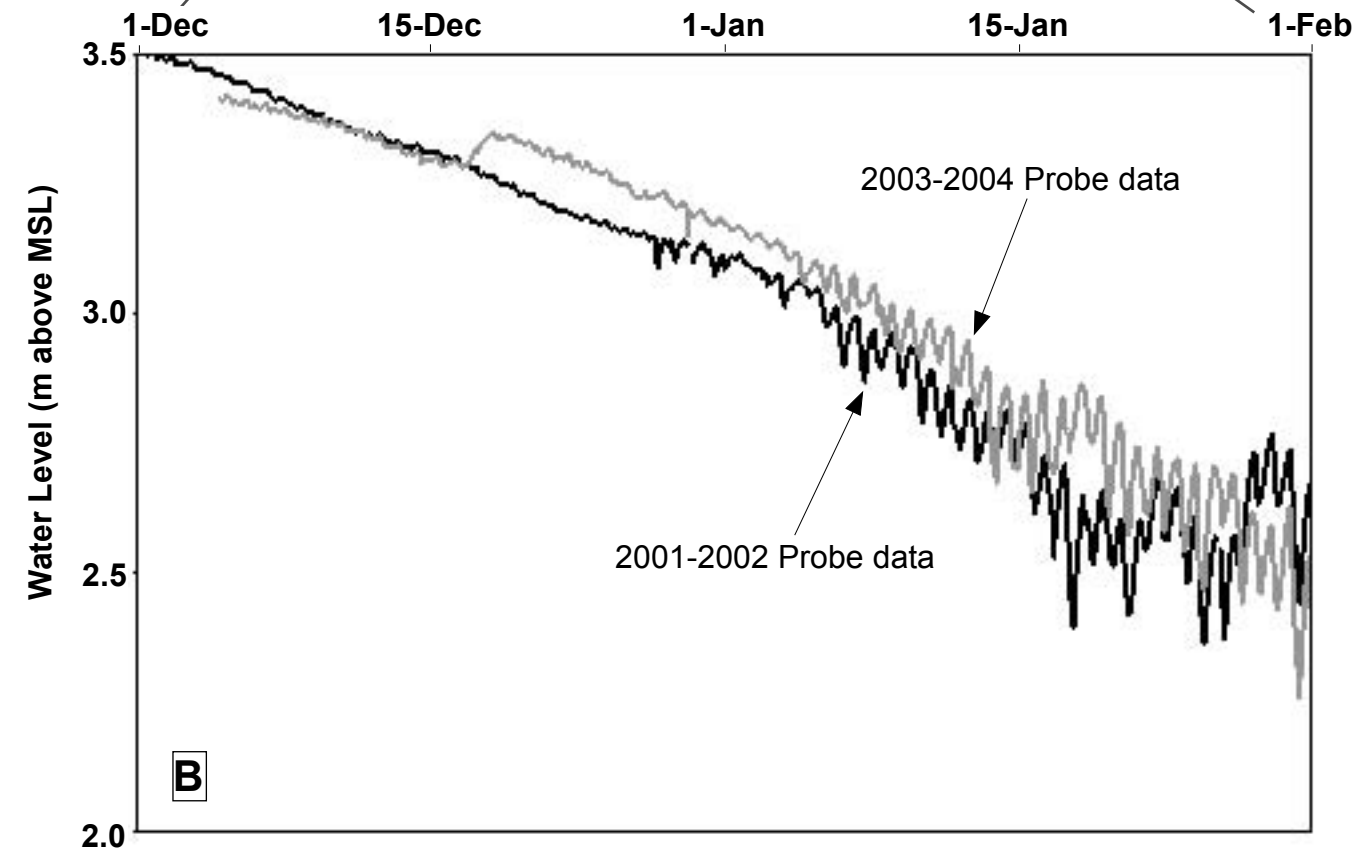
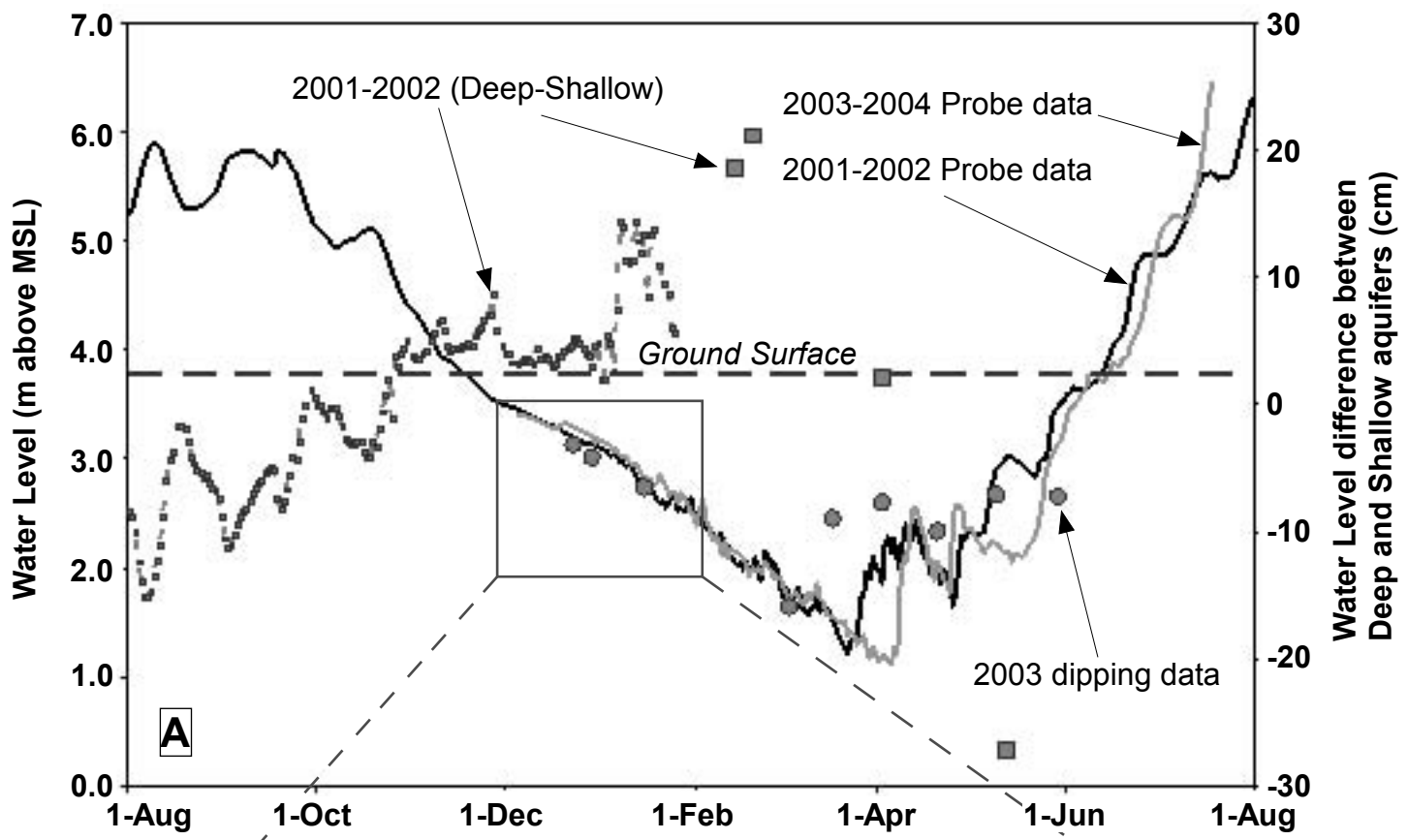


Fig.5

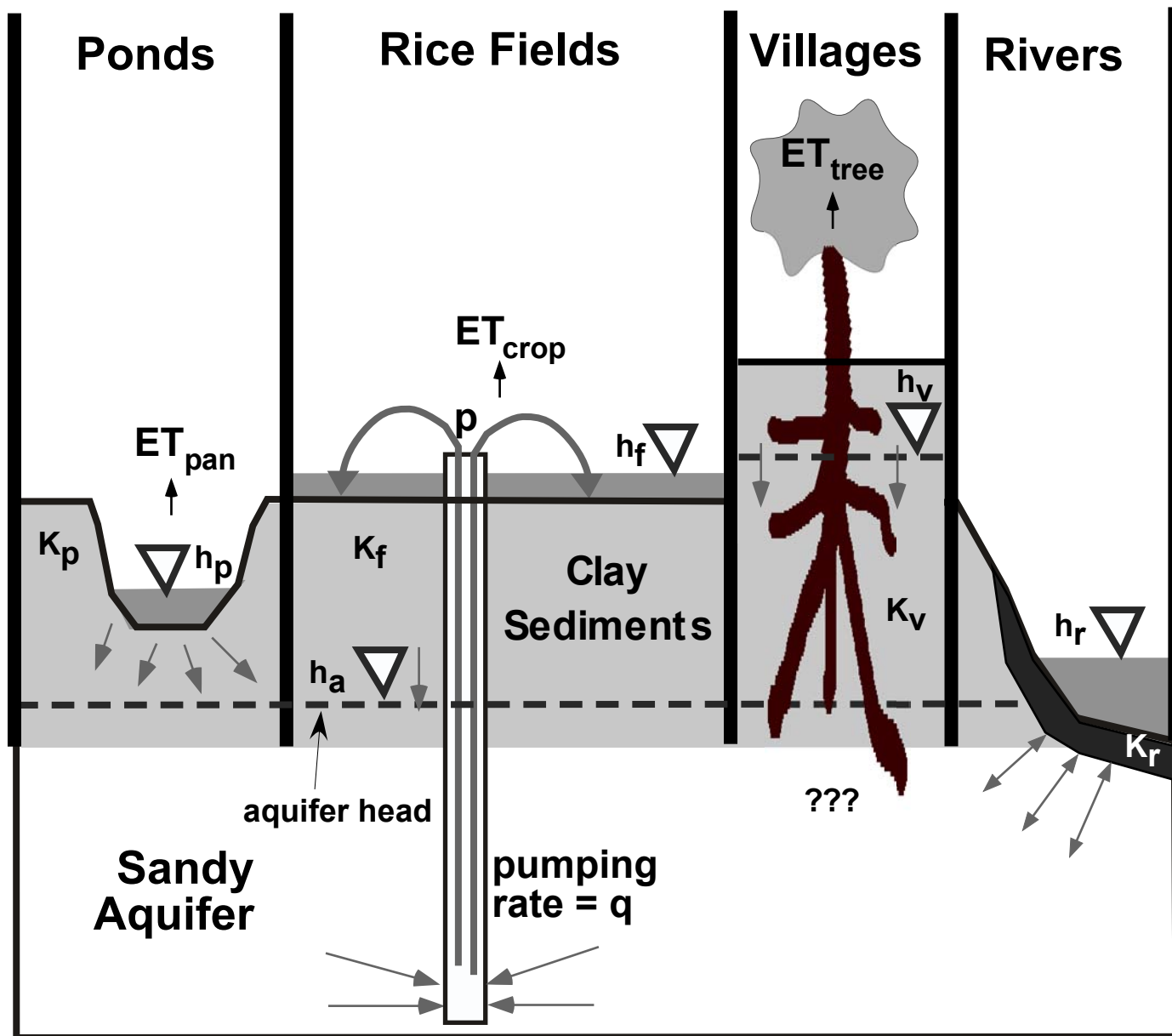


Fig.6

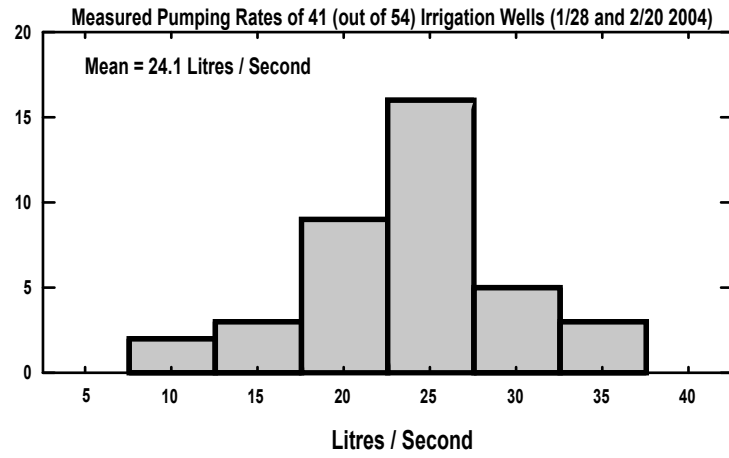


Fig.7

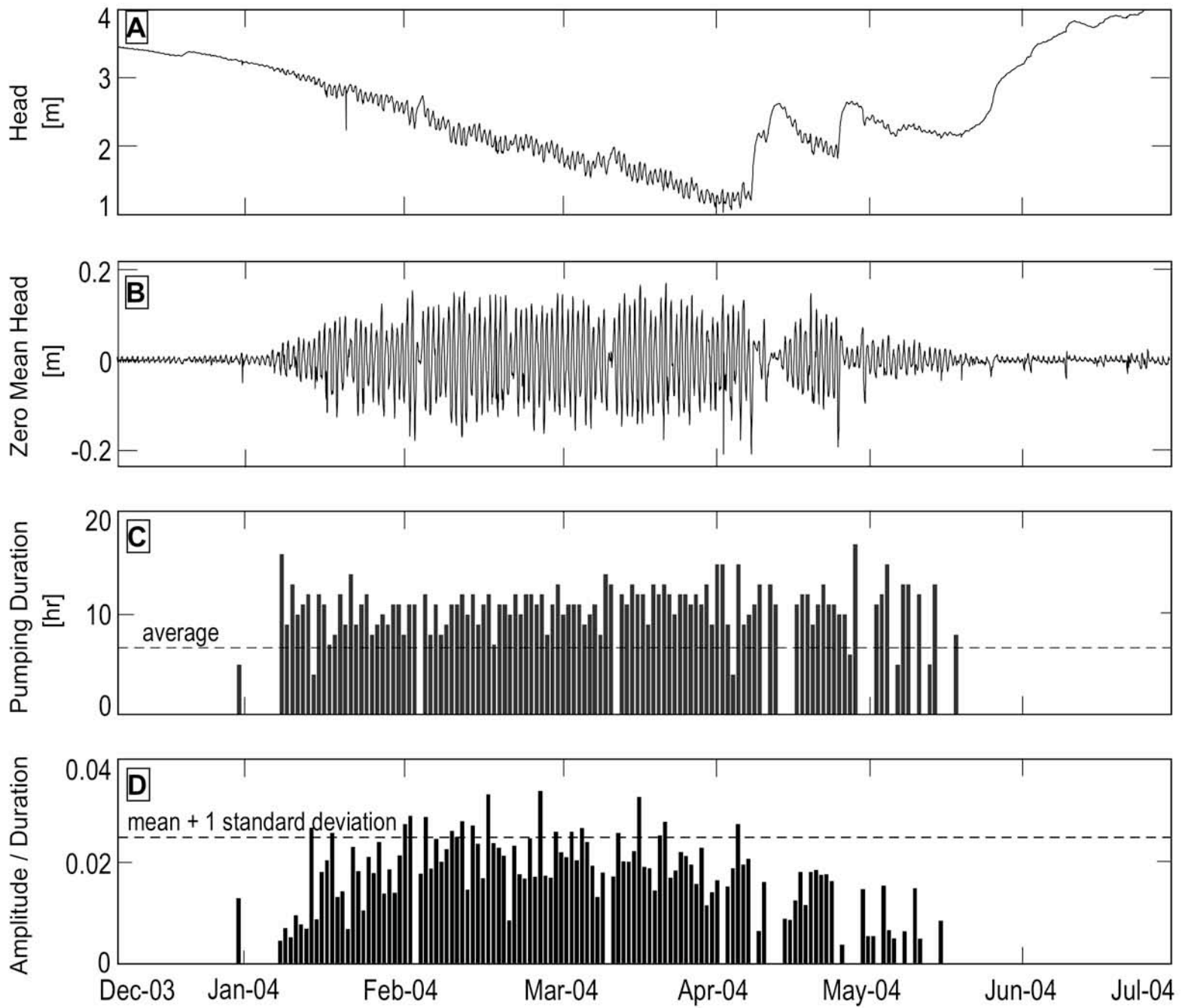


Fig.

Figure

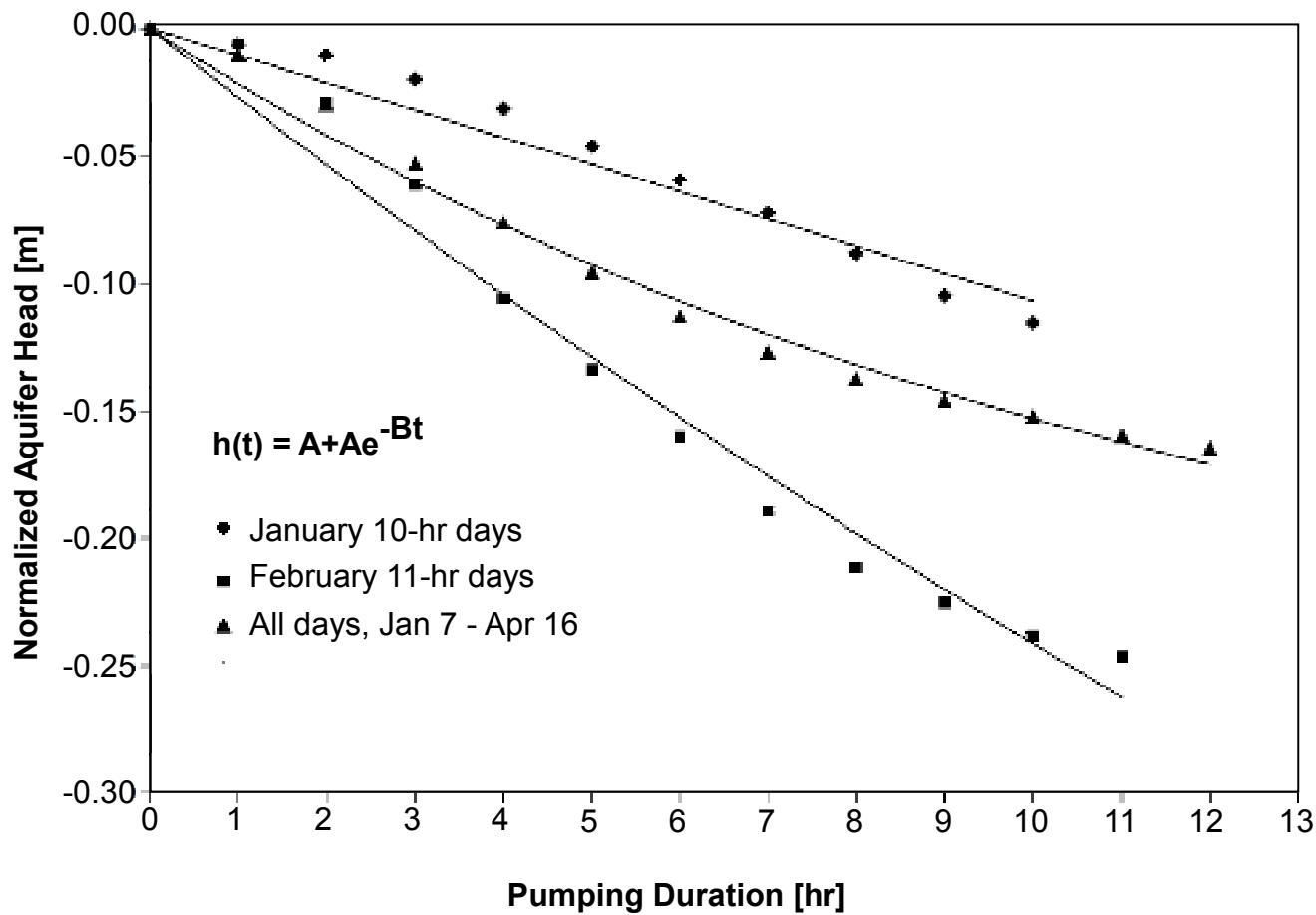


Fig.9

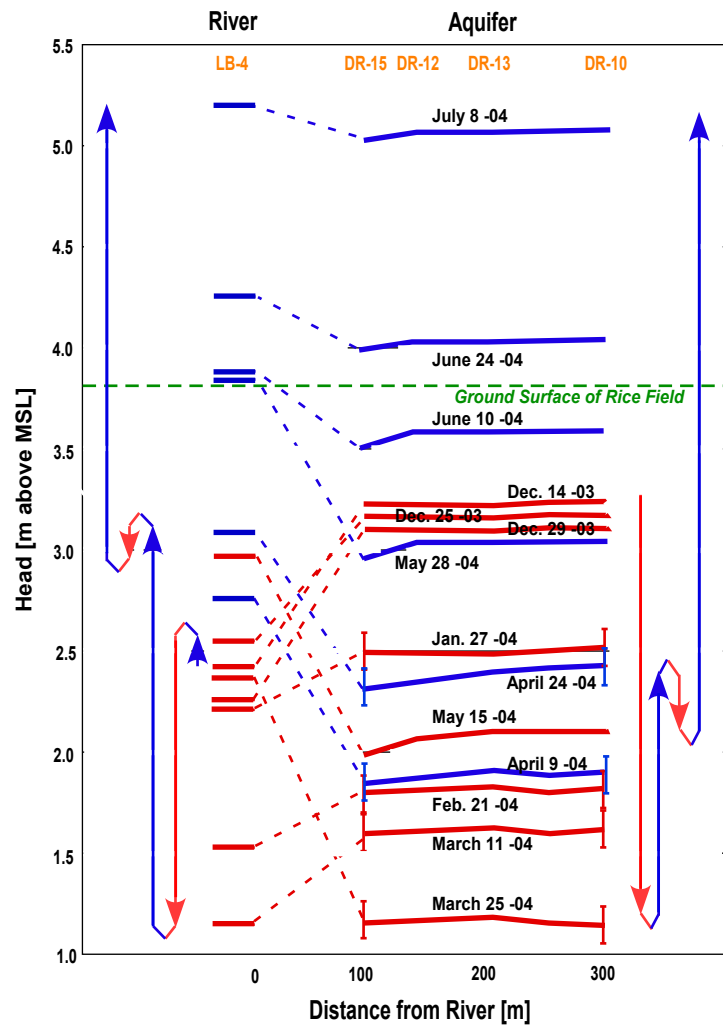


Fig.10

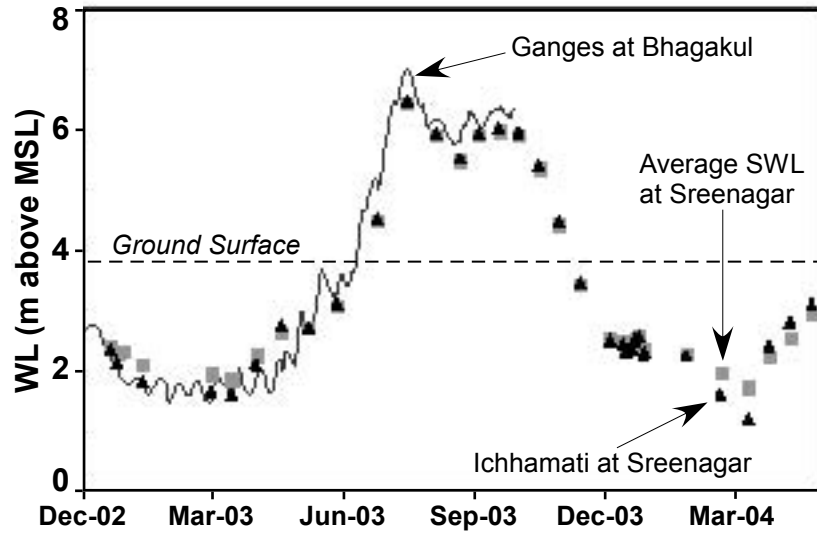


Fig.11

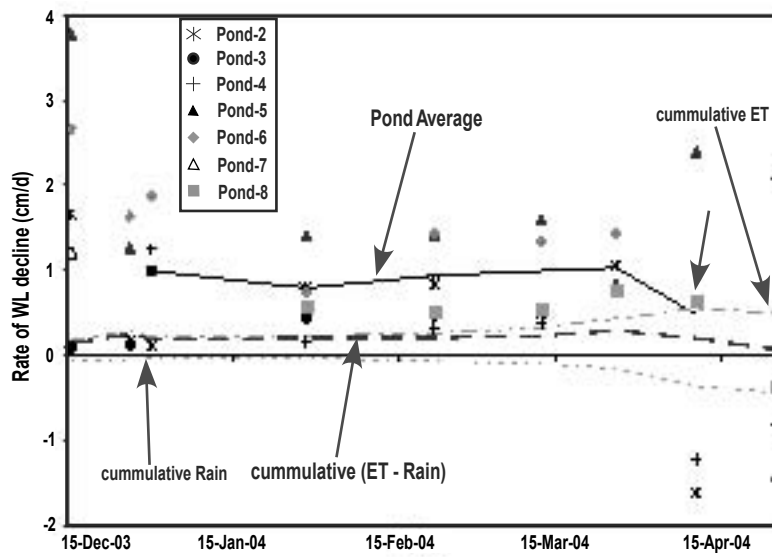
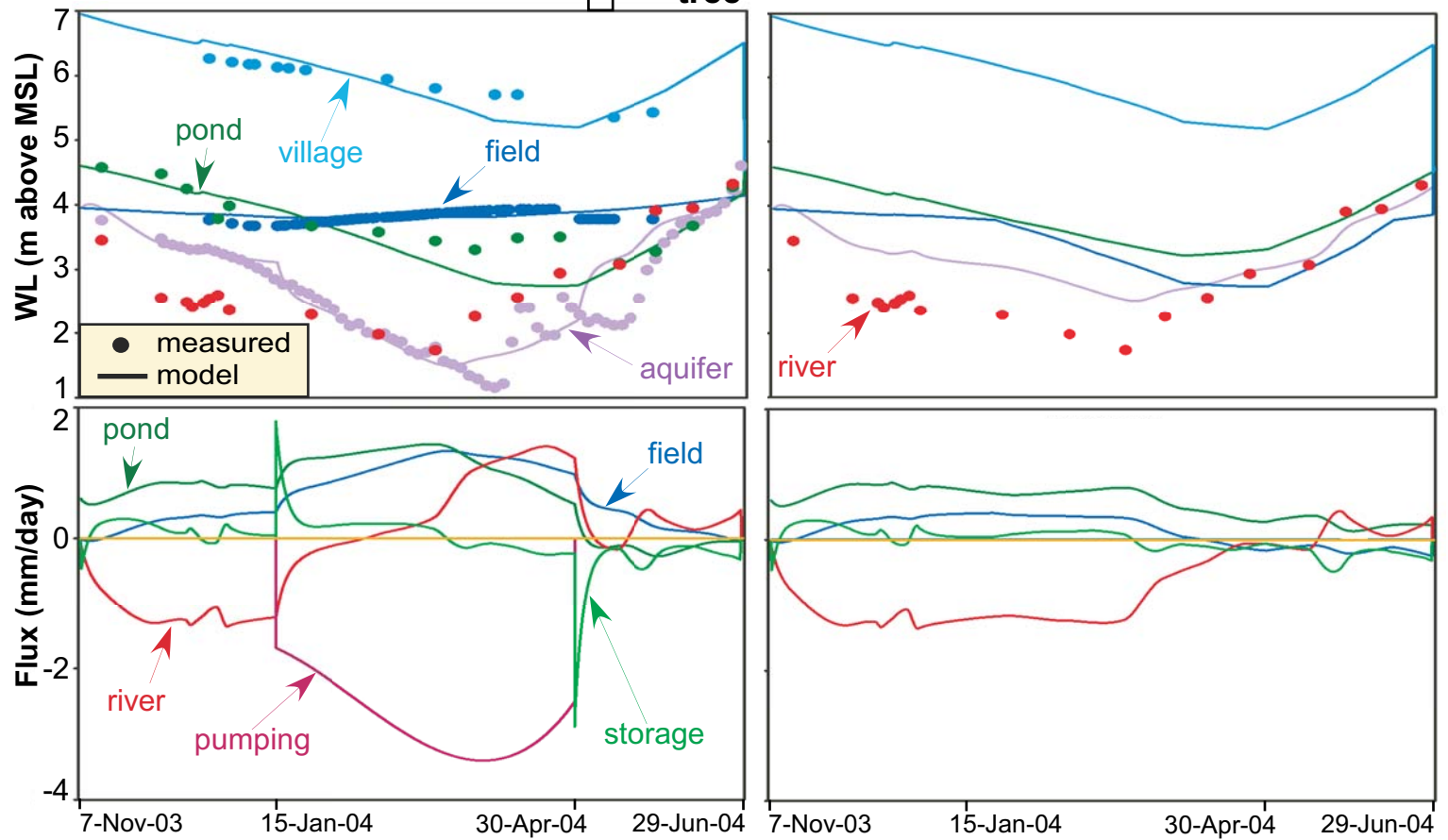


Fig.12

Estimated Heads and Fluxes with pumping

Predicted Heads and Fluxes without pumping

A: ET_{tree} from clay



B: ET_{tree} from aquifer

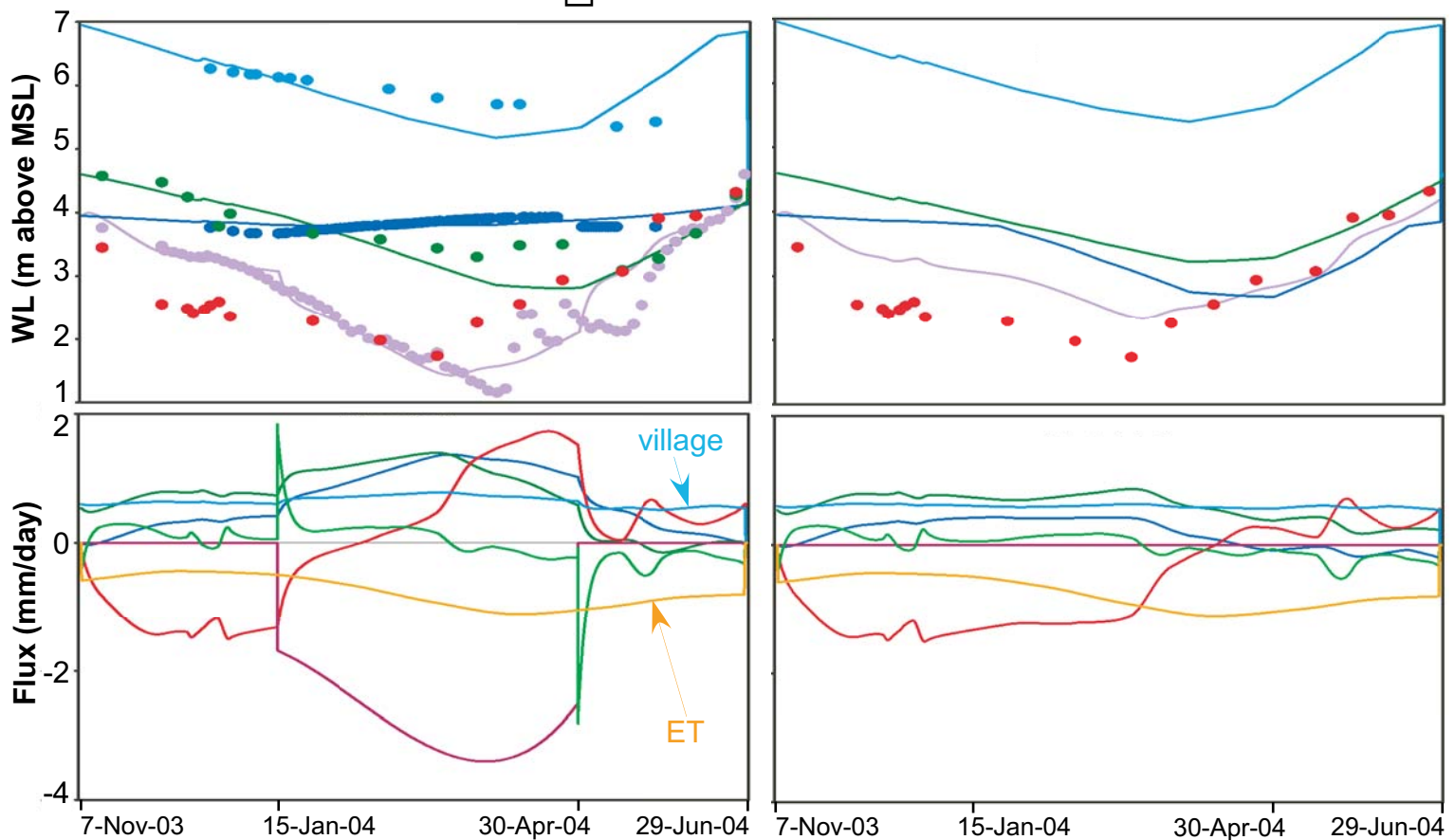


Fig.13

Case A: tree ET from clay

Case B: tree ET from aquifer

discharge *recharge*

discharge *recharge*

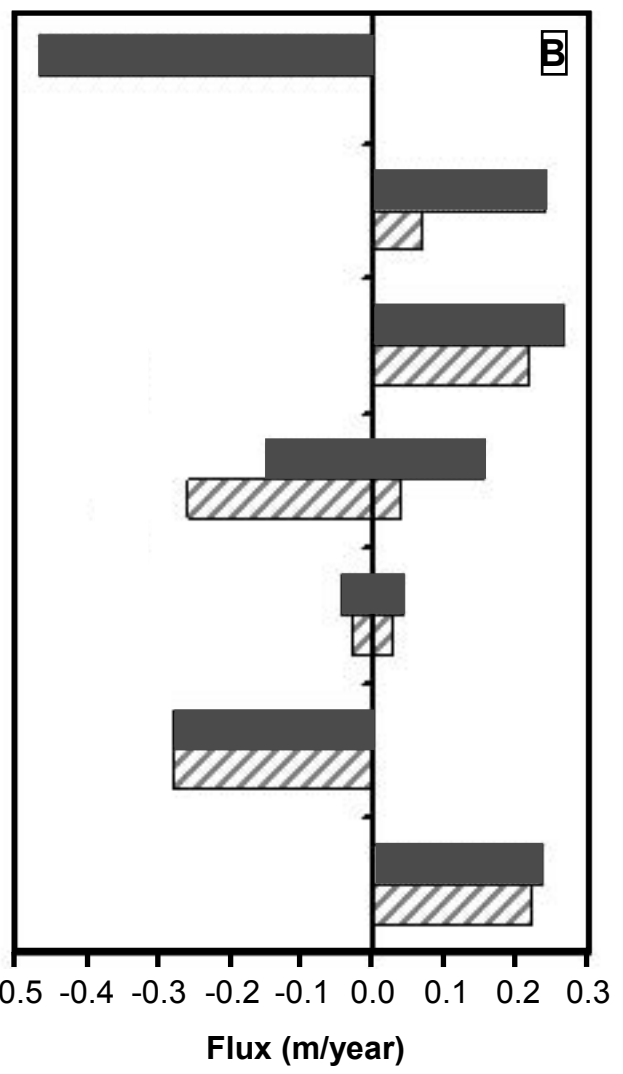
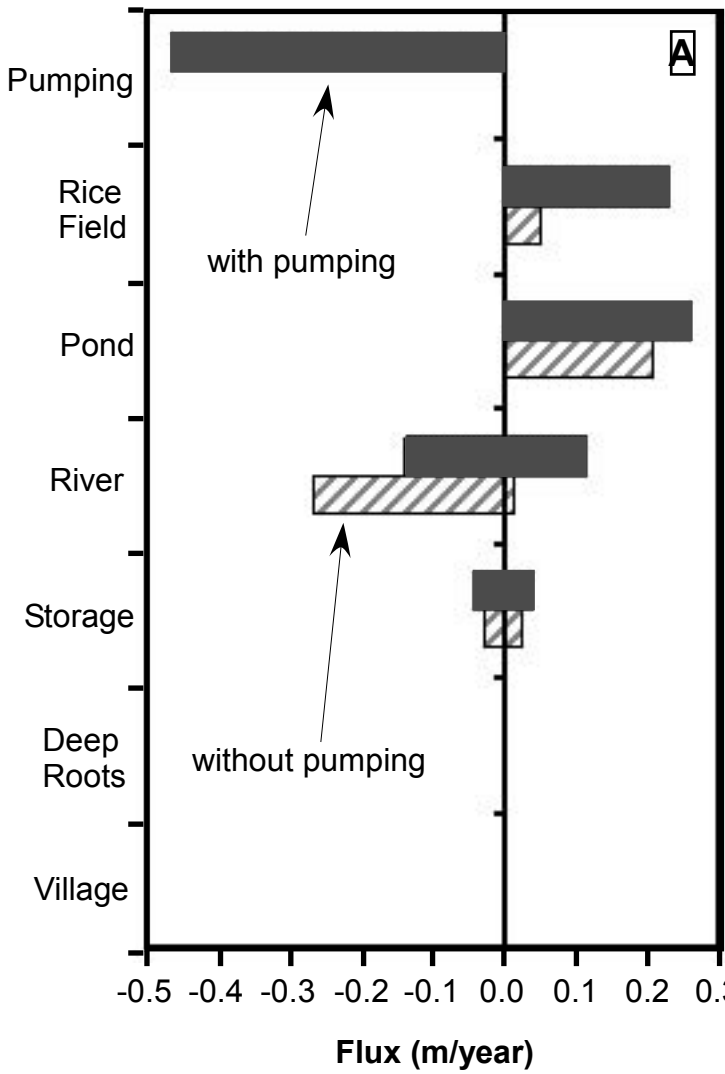


Fig.14